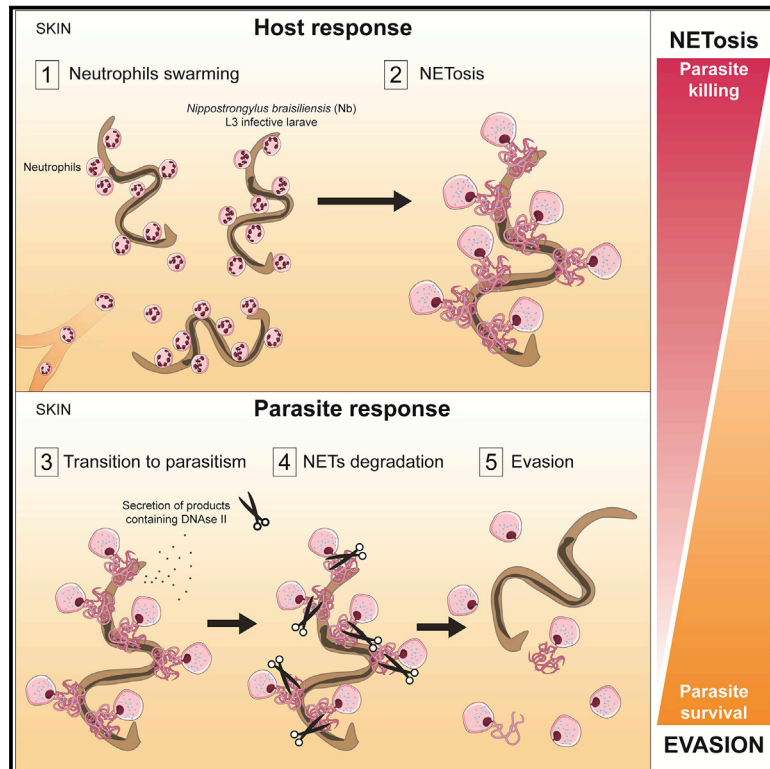


Cell Host & Microbe

Hookworms Evade Host Immunity by Secreting a Deoxyribonuclease to Degrade Neutrophil Extracellular Traps

Graphical Abstract



Authors

Tiffany Bouchery, Mati Moyat, Javier Sotillo, ..., Venizelos Papayannopoulos, Alex Loukas, Nicola L. Harris

Correspondence

nicola.harris@monash.edu

In Brief

Bouchery et al., demonstrate that neutrophils participate in defense against helminth by secreting neutrophil extracellular traps that are toxic to the parasite larvae. In response, the parasite has evolved an evasion strategy based on the secretion of a DNase II that degrades the DNA backbones of the traps.

Highlights

- Neutrophils swarm around hookworm larvae as they penetrate the skin
- Neutrophils generate extracellular traps (NETs) in response to hookworm larvae
- NETs can directly impair larval viability
- Hookworm larvae degrade NETs by secreting a deoxyribonuclease (DNase II)



Hookworms Evade Host Immunity by Secreting a Deoxyribonuclease to Degrade Neutrophil Extracellular Traps

Tiffany Bouchery,^{1,2,9} Mati Moyat,^{1,2,9} Javier Sotillo,^{3,4} Solomon Silverstein,¹ Beatrice Volpe,² Gillian Coakley,¹ Theodora-Dorita Tsourouktsoglou,⁵ Luke Becker,³ Kathleen Shah,² Manuel Kulagin,² Romain Guiet,⁶ Mali Camberis,⁷ Alfonso Schmidt,⁸ Arne Seitz,⁶ Paul Giacomini,³ Graham Le Gros,⁷ Venizelos Papayannopoulos,⁵ Alex Loukas,³ and Nicola L. Harris^{1,10,*}

¹Laboratory of Intestinal Immunology, Department of Immunology and Pathology, Monash University, Melbourne, VIC 3004, Australia

²Laboratory of Intestinal Immunology, SV, Ecole Polytechnique Federale de Lausanne (EPFL), Lausanne CH-1015 Switzerland

³Australian Institute of Tropical Health and Medicine, James Cook University, Cairns, QLD 4814, Australia

⁴Centro Nacional de Microbiología, Instituto de Salud Carlos III, Majadahonda, Madrid 28222, Spain

⁵Antimicrobial Defense Laboratory, The Francis Crick Institute, 1 Midland Rd, London NW1 1AT, UK

⁶Bioimaging and Optics Core Facility, École Polytechnique Fédérale de Lausanne (EPFL), Lausanne CH-1015, Switzerland

⁷Malaghan Institute of Medical Research, Wellington 6242, New Zealand

⁸Hugh Green Cytometry Centre, Malaghan Institute of Medical Research, Wellington 6242, New Zealand

⁹These authors contributed equally

¹⁰Lead Contact

*Correspondence: nicola.harris@monash.edu

<https://doi.org/10.1016/j.chom.2020.01.011>

SUMMARY

Hookworms cause a major neglected tropical disease, occurring after larvae penetrate the host skin. Neutrophils are phagocytes that kill large pathogens by releasing neutrophil extracellular traps (NETs), but whether they target hookworms during skin infection is unknown. Using a murine hookworm, *Nippostrongylus brasiliensis*, we observed neutrophils being rapidly recruited and deploying NETs around skin-penetrating larvae. Neutrophils depletion or NET inhibition altered larvae behavior and enhanced the number of adult worms following murine infection. Nevertheless, larvae were able to mitigate the effect of NETs by secreting a deoxyribonuclease (Nb-DNase II) to degrade the DNA backbone. Critically, neutrophils were able to kill larvae *in vitro*, which was enhanced by neutralizing Nb-DNase II. Homologs of Nb-DNase II are present in other nematodes, including the human hookworm, *Necator americanus*, which also evaded NETs *in vitro*. These findings highlight the importance of neutrophils in hookworm infection and a potential conserved mechanism of immune evasion.

INTRODUCTION

Hookworms, including *Necator americanus* (Na) and *Ancylostoma duodenale*, are highly successful nematode parasites that represent an evolutionarily ancient disease; evidence of infection has been found in human fossils dating between 4,000 and 7,000 years old (Araújo et al., 1988). Modern sanitation

methods have largely eradicated these parasites from developed regions. However, approximately 700 million people living in impoverished conditions remain infected, and many of them suffer from morbidity resulting from the anemia caused by nematode feeding on host blood (Hotez, 2008). While the host immune response to hookworm infection is robust, it fails to elicit protection, and individuals tend to exhibit heavier worm burdens with age (Hotez et al., 2016). No protective vaccines currently exist, and their successful development will require an improved understanding of both the host immune response and nematode biology (Allen and Maizels, 2011; Anthony et al., 2007; Hotez and Pecoul, 2010).

Neutrophils are highly abundant granulocytes that rapidly enter sites of infection, inflammation, or damage. They have long been known to contribute to pathogen resistance through multiple mechanisms including phagocytosis, production of reactive oxygen species, and the release of granules containing toxic mediators. More recently, activated neutrophils were observed to release extracellular nucleic acids decorated with histones and granular proteins, termed neutrophil extracellular traps (NETs) (Brinkmann et al., 2004). Since their discovery, a large body of research has demonstrated that neutrophils actively form NETs (a process known as NETosis) in response to an array of pathogens—including bacteria, fungi, viruses, and protozoa (Yipp and Kubers, 2013). Evidence that NETs can provide defense against pathogens has also been demonstrated for *E. coli* (McDonald et al., 2012), *Staphylococcus* (Yipp et al., 2012), *Candida albicans* (Byrd et al., 2013; Urban et al., 2006), and HIV (Saitoh et al., 2012). Interestingly, NETs have been shown to be deployed selectively against pathogens that are too large to be killed intracellularly, such as fungal hyphae, and play a critical role in their clearance (Branzk et al., 2014). Several groups have now reported formation of NETs around other large pathogens, including



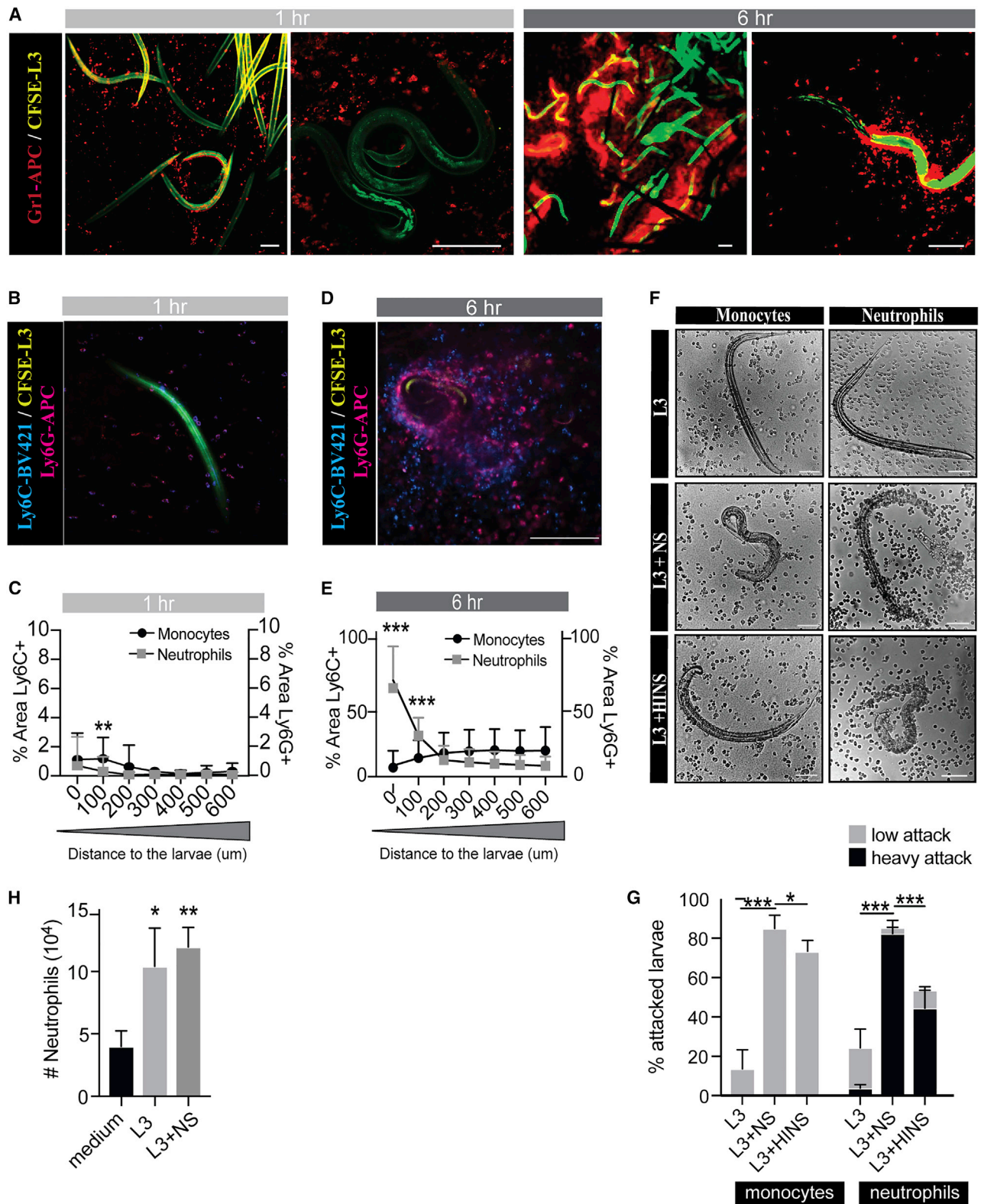


Figure 1. Myeloid Cells Form Swarms around Skin Penetrating Hookworm Larvae

(A–E) Mice were injected with the indicated labeled mAb(s) intravenously (i.v.) 1 h before intradermal (i.d.) injection of 250 CFSE-labeled Nb L3 into the belly skin. At 1 and 6 h following infection mice were sacrificed, the infected skin removed, and imaging performed as described in Figure S1A. Data were collected from 2 independent experiments (n = 3–5 mice/time point) and representative images are shown. Scale bar, 100 μ m. (A) Mice received 10 μ g APC-labeled anti-Gr1 mAb (legend continued on next page)

nematodes (Díaz-Godínez and Carrero, 2019; McCoy et al., 2017; Mendez et al., 2018; Muñoz-Caro et al., 2015; Pellegrines et al., 2017; Tamarozzi et al., 2016), however, a functional role for NETs in anti-nematode defense has not been demonstrated.

Nippostrongylus brasiliensis (Nb) is a well-studied rodent helminth that is closely related to human hookworm. Infective larvae (L3) penetrate the skin of their hosts and here they must undergo maturation from a free-living to a parasitic stage (Datu et al., 2008). At some point during this process, they also shed their residual cuticle (i.e., exsheath; Rogers and Sommerville, 1957), after which they enter the blood vessels and become trapped within the post-capillary venules of the lung. In the lung, they undergo a developmental molt to the L4 stage and are “coughed up” and swallowed. Larvae complete their maturation to adult worms within the small intestine, after which they mate and produce eggs that are released back into the environment through the feces. Protection against the tissue migratory stages of Nb can occur in immune-competent mice following repeated infections and typically involves the production of type 2 cytokines that function to recruit and stimulate macrophages that attack the larvae in the lungs (Bouchery et al., 2015; Chen et al., 2014; Knott et al., 2007) or in the skin (Obata-Ninomiya et al., 2013). Neutrophils have also been shown to be required for protection against reinfection by contributing to type 2 cytokine production (Chen et al., 2014). Neutrophil and eosinophil recruitment have previously been reported in air pouches containing Nb, where eosinophils were shown to contribute to worm killing (Giacomin et al., 2008). Whether neutrophils provide innate resistance against these parasites remains unclear, although recent reports indicate a potential role for neutrophils in killing larvae within the lung (Sutherland et al., 2014).

In the current study, we set out to determine which cells respond to the initial encounter with infective hookworm larvae in the skin and to assess the possible contribution of these cells to host defense. Monocytes and neutrophils were rapidly recruited toward hookworm larvae following skin invasion; large numbers of neutrophils were observed adhering to the surface of the larvae. The presence of neutrophils around larvae altered larval exsheathment and migration and led to an increased number of surviving adult worms in the small intestine. More extensive analyses revealed that NETs played a crucial role in this process and that hookworms have evolved a previously unrecognized evasion mechanism involving the secretion of a DNase II able to degrade the DNA backbone of NETs.

RESULTS

Hookworm Infection of the Skin Elicits Rapid Neutrophil Swarming

Myeloid cell recruitment from the blood to extravascular sites of tissue damage is a hallmark of the early innate immune response. To assess the possible recruitment of myeloid cells into the skin following Nb infection, we injected mice with allophycocyanin (APC)-labeled anti-Ly6G/Ly6C (Gr1) mAb (monoclonal antibody), followed by infection with carboxyfluorescein succinimidyl ester (CFSE)-labeled L3 delivered via intradermal injection. Myeloid (Gr1⁺) cell recruitment and larvae were then visualized using confocal imaging of excised tissue (Figure S1A). Myeloid cells rapidly accumulated at the site of infection and formed swarms around the larvae by 6 h post-infection (Figure 1A). To determine the relative contribution of monocytes or neutrophils to the swarms, we utilized labeled antibodies specific for neutrophils (anti-Ly6G) or monocytes (anti-Ly6C), and then determined the proximity of each cell type to larvae using a custom-made script as detailed in Figures S2 and S1B. Both neutrophils and monocytes began to accumulate around larvae by 1 h post-infection (Figures 1B and 1C). At 6 h post-infection, swarms of neutrophils were observed in close proximity to larvae, while monocytes were predominant at the outer edges of the swarm (Figures 1D and 1E). At 1 h post-infection, larvae are still within their outer sheath (Figure S1C), but by 6 h, larvae were motile and had begun to exsheath (Figure S1D). By 13 h, the majority of larvae had left the skin and mainly empty sheaths remained (Figure S1E). Of note, the few larvae that did remain at this time point were consistently surrounded by large swarms of neutrophils (Figure S1E).

Although experimental infection with Nb is typically performed by injection of infective larvae, natural infections occur via skin penetration following exposure of the host to larvae present in the soil. We therefore addressed whether myeloid cell recruitment to larvae also occurred during a natural infection. For this purpose, we administered CFSE-labeled L3 via topical application to the belly skin of mice previously injected with APC-labeled anti-Gr1 antibody. Mice were subjected to repeated topical applications of larvae until a final dose of 100 L3 was reached, then sacrificed 1 h later. By this time, the majority of larvae penetrating the skin were surrounded by Gr1⁺ cells (Figure S1F), indicating that myeloid cell recruitment around larvae also occurs in response to natural infection. However, because of the low efficiency of the skin penetration by Nb (approximately 8% of total larvae applied) and the need for repeated topical applications, we returned to the use of intradermal injections for all subsequent experiments.

i.v. Images show larvae (green) and myeloid cells (red). (B and D) Mice received 5 μ g APC-labeled anti-Ly6G mAb and 5 μ g BV421-labeled anti-Ly6C mAb i.v. Images show larvae (green), monocytes (blue), and neutrophils (pink). (C and E). Monocytes and neutrophils surrounding larvae were quantified using a custom macro (Figure S2) and the distance of each cell from the larvae determined as described in Figure S1B.

(F) 100 Nb L3 were co-cultured for 24 h with 1 million neutrophils or monocytes freshly isolated from the bone marrow of naive mice. Naive serum (NS) or heat-inactivated serum (HINS) were added to the cultures. DIC-images were acquired using a brightfield microscope and representative images are shown from a total of 3 independent experiments (n = 5 wells/condition). Scale bar, 100 μ m.

(G) The percentage of attacked larvae was calculated for each well of the cultures described in (F). The efficiency of cellular adherence is shown as low (<20 cells/larvae) or high (>20 cells/larvae). Data were pooled from a total of 2 independent experiments (n = 5 wells/condition) and analyzed by two-way ANOVA.

(H) Chemotaxis assays were performed using neutrophils freshly isolated from the bone marrow of naive mice placed in the upper chamber of a transwell with 150 Nb L3 (with or without additional naive serum) placed in the lower chamber, and the number of neutrophils that had migrated to the lower chamber determined at 24 h. Data were collected from 2 independent experiments (n = 3 wells/condition) and analyzed by ANOVA.

Myeloid cell recruitment around skin larvae could occur in response to the presence of larvae or as a consequence of tissue damage resulting from larval migration. We predicted that neutrophils could respond directly to larvae, because *in vivo* injection of killed larvae elicited extensive neutrophil swarming, while sham injections did not (Figures S1G and S1H). To test this hypothesis, we co-cultured neutrophils or monocytes together with larvae *in vitro*. After 24 h, both neutrophils and monocytes adhered to larvae, with the addition of serum increasing adherence in a manner that was partly dependent on complement (Figures 1F and 1G). Of note, the monocyte-mediated attack was less dramatic than the neutrophil attack (Figure 1G). The addition of serum also resulted in larger numbers of adhering neutrophils compared with monocytes, mimicking our *in vivo* observations (Figures 1F and 1G). Interestingly, the attraction of neutrophils toward larvae occurred in a chemotactic manner as demonstrated using a transwell system (Figure 1H), however, this process was serum independent.

Hookworm Larvae Adapt Their Development after Sensing Neutrophils

To determine whether the myeloid cells that surrounded skin penetrating larvae impacted on their survival, we depleted both neutrophils and monocytes using anti-Gr1 mAb, or only neutrophils using anti-Ly6G mAb, then determined the number of larvae that were able to exit the skin and migrate to the lung. The efficiency of cell depletion was confirmed by visualizing cellular recruitment around skin larvae (Figure S3A).

In mice depleted of neutrophils, or neutrophils and monocytes, a smaller number of larvae were observed to reach the lung by 24 h post-infection (Figures 2A and S3A). However, by 48 h this difference was reduced, indicating that the presence of neutrophils acted mainly to delay larval migration from the skin to the lung (Figure 2A). A quantitative analysis of the number of larvae present in the skin of mice was not possible, however, we were able to determine whether neutrophils impacted on larval behavior as determined by the process of larval exsheathment. For this purpose, we labeled the sheath of the larvae with CFSE and the internal larvae with yellow orange (YO) carboxylate microspheres. Sheathed larvae could be observed as yellow, while exsheathed larvae were red and empty sheaths were green (Figure 2B). An analysis of the skin injection site of mice treated with the neutrophil-depleting or isotype control mAb was then conducted at 1 and 6 h post-infection. At 1 h post-infection the majority of larvae were still within their sheaths in both groups of mice (Figure S3B). By 6 h post-infection, larval exsheathment had begun, and a greater proportion of exsheathed versus sheathed larvae were present in mice treated with neutrophil-depleting compared with isotype control mAb (Figures S3B, 2B, and 2C). Finally, by 13 h post-infection, very few sheaths or exsheathed larvae could be observed at the injection site of mice treated with the isotype control mAb, while both sheaths and exsheathed larvae in the mice depleted of neutrophils (Figure S3B). Collectively, these data indicated that larvae respond to the presence of neutrophils by staying within their sheaths longer and by traveling more quickly to the lungs once they do exsheath. The ability of larvae to respond to the presence of neutrophils was also addressed using an *in vitro* co-culture system. In these experiments, $14.83\% \pm 3.8\%$ of larvae cultured

at 37°C underwent exsheathment after 24 h (Figure 2D). However, when neutrophils were added to the culture, only $4.9\% \pm 1.5\%$ of larvae underwent exsheathment (Figure 2D), confirming that larvae respond to the presence of neutrophils by remaining within their sheaths for a longer period of time. We next determined whether the altered behavior of larvae in the presence of neutrophils impacted on the development of adult worms within the intestine. The depletion of neutrophils, or neutrophils and monocytes, during the early stages of the infection resulted in a larger number of adult worms at day 5–6 post-infection, which represents the time point when expulsion normally begins to occur and just prior to egg production (Figure 2E).

Excretory and Secretory Products of Hookworm Larvae Degrade NETs

Our data indicated that neutrophils can impact negatively on larval fitness, and we reasoned that one of the means by which they could achieve this could be by forming NETs around the larvae. We therefore addressed whether neutrophils could undergo NETosis in response to larvae using the *in vitro* co-culture assay of neutrophils plus larvae, in which we assessed DNA release from the neutrophils using the cell impermeable DNA dye, Sytox. Following 1 h of co-culture with live larvae, no extracellular DNA could be detected, indicating that NETs were not present (Figure 3A). Interestingly, however, extracellular DNA was present in co-cultures of neutrophils and dead larvae (Figure 3A). Despite its ability to enhance neutrophil adherence to larvae, the addition of serum resulted in a reduction in extracellular DNA present in cultures containing either live or dead larvae, similar to what has been recently reported for LPS-induced NETs (Figure 3A; Neubert et al., 2018). To validate that the extracellular DNA originated from NETs, we stained for citrullinated histones (H3) and the granule protein myeloperoxidase (MPO), which are specific NET markers. The cultures with dead larvae contained MPO⁺ and H3⁺ neutrophils and exhibited clear evidence of extracellular staining for the same proteins, indicating that NETosis had occurred, with NETs still visible (Figure 3B). Neutrophils in the cultures containing live larvae did not exhibit extracellular staining for these proteins, confirming that NETs were not present. Of note, however, these neutrophils did exhibit positive intracellular staining for both proteins, suggesting that NETs may have formed but were subsequently degraded (Figure 3B).

The observation that NETosis occurs in response to both live and dead larvae, but that NETs could only be detected in cultures of dead larvae, suggested that live larvae may secrete a DNase capable of degrading the DNA backbone of NETs. Infective larvae respond to the 37°C temperature of their hosts and the presence of serum components by actively secreting enzymes that function to facilitate migration, promote feeding, and modulate host immune responses (Datu et al., 2008; Hawdon and Schad, 1990; Weinstein and Jones, 1956). To determine whether the excretory secretory products of Nb infective larvae (NES) also contain enzyme(s) with DNase activity, we tested the ability of NES to degrade NETs formed in response to *Candida albicans* hyphae. Neutrophils were activated by *C. albicans* hyphae and NET formation was assessed dynamically using time-lapse microscopy. In the absence of NES, NETs were visible from the time of formation for at least 6–11

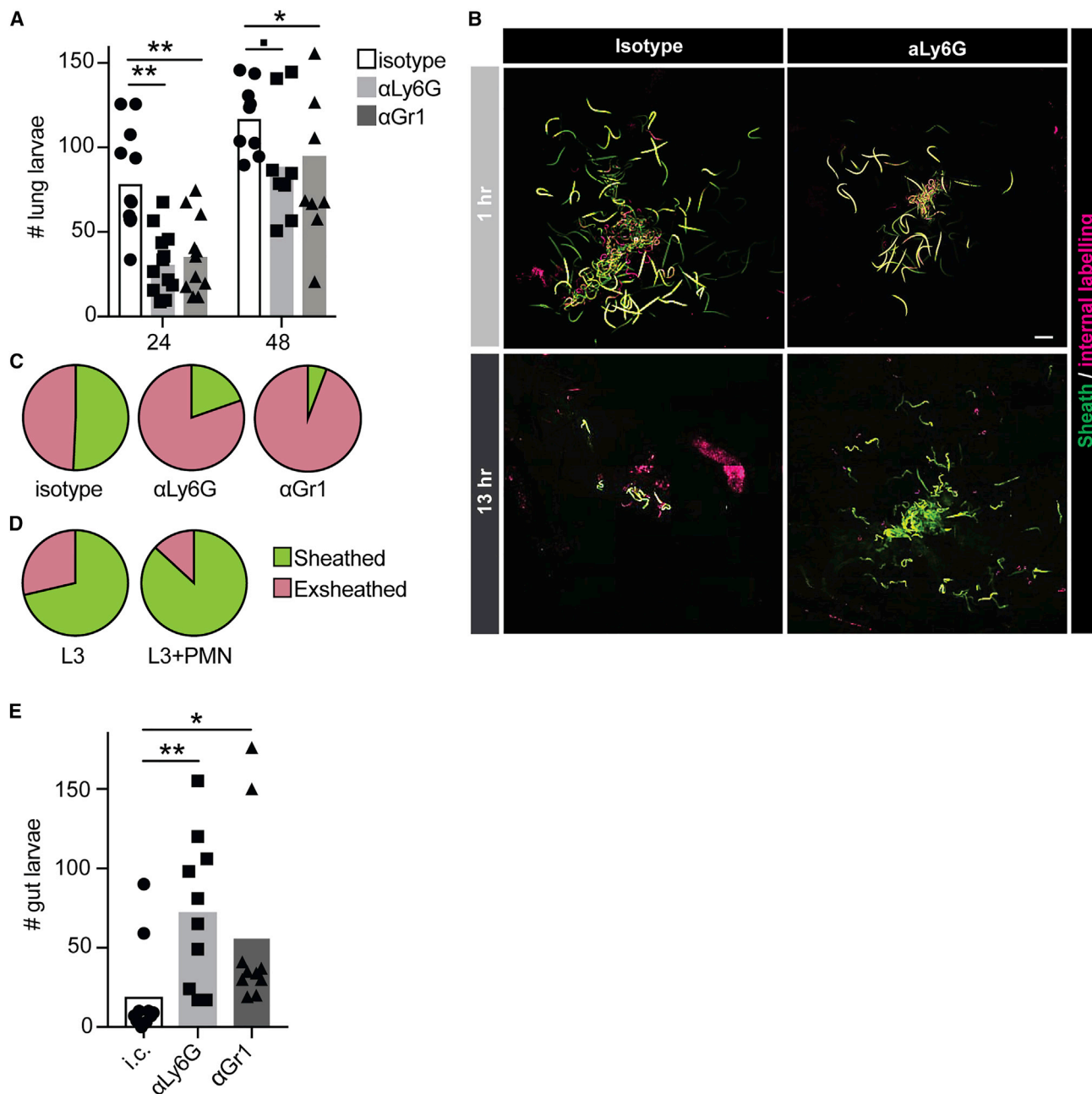


Figure 2. Hookworm Larvae Sense Neutrophils and Adapt Their Development to Their Presence

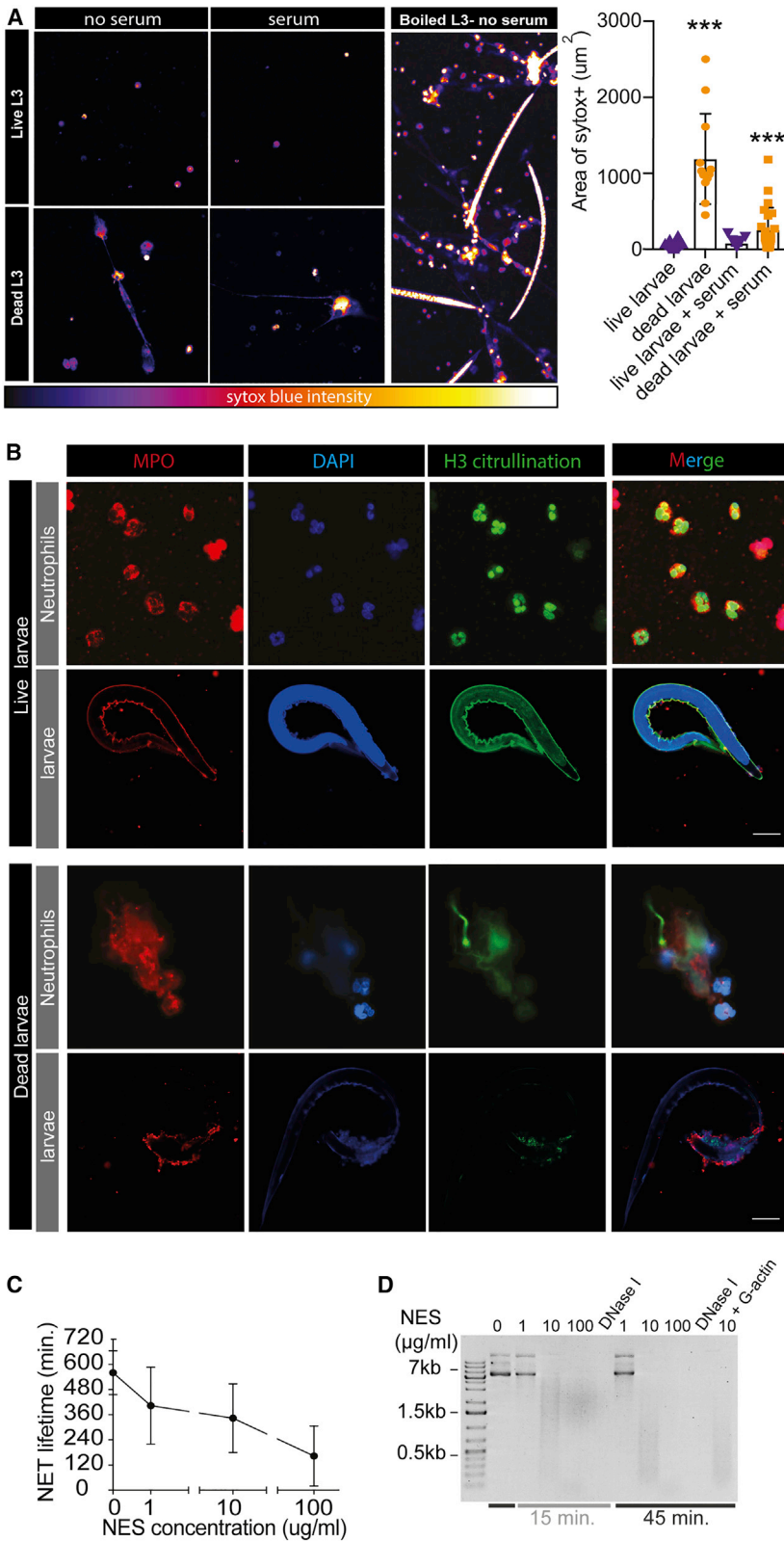
(A) Mice were treated with 250 μ g anti-Gr1 mAb or 500 μ g of anti-Ly6G mAb by intraperitoneal (i.p.) injection and day -1 , 0 , and 1 . On day 0 , mice were infected with 250 antibiotic-treated Nb L3 by i.d. injection and skin and lungs removed 24 and 48 h later. Data are pooled from 2 independent experiments ($n = 8-10$ /group) and analyzed by ANOVA.

(B and C) Mice were treated with anti-Gr1 mAb and anti-Ly6G mAbs, as for (A), and infected with 250 doubled-labeled L3 (CFSE for external labeling, yellow orange (YO) carboxylate microspheres for internal labeling) in the belly skin. The dispersion of larvae was determined in the skin at 6 h following infection by mounting excised skin in a chamber containing fluorobrite medium at 37°C under 5% CO_2 stimulation. The skin was imaged from the inside (subcutaneous tissue) with a confocal microscope. Scale bar, 400 μm . Images are representative of 2 independent experiments ($n = 3$ mice/time point).

(C) The percentage of sheathed versus exsheathed larvae was enumerated and data analyzed by ANOVA. Bonferroni multiple comparisons show significant changes for isotype control versus Gr1-mAb-treated groups ($p = 0.0006$) and isotype control versus Ly6G-mAb-treated groups ($p = 0.0113$).

(D) Nb L3 were cultured in the presence or absence of neutrophils and the percentage of sheathed versus exsheathed L3 determined after 24 h using a brightfield microscope. Data are representative of 4–5 independent counts of 100 L3 and analyzed by a t test ($p = 0.034$).

(E) Mice were treated with depleting mAb and infected with L3, as for (A), and the number of worms in the intestine determined 5 days later. Data are pooled from 2 independent experiments ($n = 8-10$ mice/group) and analyzed by ANOVA.



h. Remarkably, the presence of NES did not impact the formation of NETs (Figure S4A)—however, it did impact in a dose-dependent manner the half-life of NETs, indicating that NES promotes NET degradation (Figure 3C). NES also resulted in the degradation of plasmid DNA, in a time- and dose-dependent manner, confirming the presence of DNase activity (Figure 3D). Interestingly, G-actin, a known inhibitor of DNase I, did not inhibit the DNA-degrading activity of NES, suggesting that the NES DNase is structurally different to DNase I (Figure 3D). A recent study reported that *Staphylococcus aureus* subverts host immunity by secreting nucleotidases that degrade NETs, leading to the release of factors toxic for surrounding monocytes (Papayannopoulos, 2014; Thammavongsa et al., 2013). We therefore assessed whether NES-mediated degradation of NETs also impacted on monocyte viability, however, we were unable to find any evidence of toxicity in this setting (Figure S4B).

To determine whether degradation of NETs by live larvae also occurs *in vivo*, we subjected mice previously injected with Sytox to intradermal injection of live or dead larvae and determined the presence of NETs within the skin. At 3 h post-infection, a small amount of extracellular DNA surrounded both live and dead larvae (Figure 4A). However, by 6 h, extracellular DNA could only be found in close contact to dead larvae and was virtually absent from the skin containing live larvae, despite the presence of neutrophils in both settings (Figure 4A). These observations suggested that larvae can secrete a DNase capable of degrading the DNA backbone of NETs *in vivo*. In support of this hypothesis, the presence of extracellular DNA around dead larvae could be prevented by co-injection of dead larvae together with NES (Figure 4B). This effect was similar to that observed by pre-treatment of mice with a recombinant DNase I (Figure 4B), a protocol widely used to facilitate NET degradation.

The observed ability of Nb infective larvae to degrade NETs suggested an evolutionary advantage of this process, perhaps as a means to prevent larval damage inflicted by NETs. To address this, we treated mice with a recombinant DNase I intraperitoneally at repeated intervals during the first 12 h following infection. Similar to what was observed after neutrophil depletion, less larvae were found in the lungs of treated mice at 48 h post-infection (Figure 4C), and an increased number of adults were recovered from the intestine at day 5–6 following infection (Figure 4D). We confirmed the role of NETs in altering parasite viability using protein arginine deiminase 4 (PAD4)-deficient mice and by treating mice with a neutrophil elastase (NE) inhibitor (Yanagihara et al., 2007) to prevent neutrophils from undergoing NETosis. In both cases, a reduced number of larvae were observed in the lung at 48 h post-infection (Figure 4E).

Hookworm Larvae Secrete a DNase II to Escape Larval Killing by NETs

We next set out to identify the protein(s) harboring DNase activity within NES. As the DNase activity in NES was not inhibited by G-actin, we searched for a DNase II motif in the sequences of identified proteins secreted by the L3 stage of Nb (Sotillo et al., 2014) and identified one protein, m.13872 (hereafter called Nb-DNase II; Data S1; Figure 5A). A blast search of NCBI non-redundant protein sequences indicated that Nb-DNase II is highly conserved within clade VI nematodes including *Ancylostoma*

ceylanicum, *N. americanus* (Na, human hookworms), *Haemonchus contortus* and *Trichuris muris* (sheep roundworms), and *Heligmosomoides polygyrus bakeri* (murine hookworm) (Figure 5A). Interestingly, Nb-DNase II is more highly expressed in the L3 than the adult worms, suggesting an evasion strategy tailored for the transition of early-stage infection to parasitism (Sotillo et al., 2014).

We next produced a recombinant form of Nb-DNase II in *E. coli* and tested the ability of the recombinant protein (rNb-DNase II) to degrade NETs formed *in vitro* by neutrophils stimulated with phorbol 12-myristate 13-acetate (PMA). The addition of rNb-DNase II resulted in degradation of NETs in a manner similar to that observed for NES (Figure 5B). We also generated an anti-serum against rNb-DNase II and demonstrated that the addition of this anti-serum to PMA-stimulated neutrophils could reverse NES-mediated degradation of NETs, while naive serum could not (Figure S5A). The ability of the anti-serum to block NET degradation by NES allowed us to assess the impact of intact NETs on larval viability. To this end, we added Sytox (a dye to which the cuticle of live larvae is impermeable) to larval neutrophil co-cultures, with or without anti-serum, and counted the proportion of larvae that took up the dye. The presence of neutrophils alone led to an increased proportion of Sytox⁺ larvae, indicating that these cells could directly kill the parasite (Figure 5C). Of note, addition of the anti-serum to block the ability of larvae to secrete DNase II resulted in increased larval killing, providing direct evidence that NETs function to impair parasite survival (Figure 5C).

Given that we had identified several putative homologs of Nb DNase II in the Na proteome (Figure 5A), we next aligned the sequence of those putative homologs and found that the two catalytic sites specific of DNase-II were highly conserved, with XP_013307665 presenting the greatest identity (63.39%) (Figure S5B).

These data indicate that Na larvae may also secrete a DNase II capable of degrading NETs. To address this experimentally, we co-cultured live or dead Na larvae together with neutrophils *in vitro* and assessed the presence of NETs using Sytox staining. NETs were observed more often in association with dead larvae as compared with live larvae, indicating that live larvae are able to degrade NETs (Figure 5D). We next confirmed that the observed extracellular DNA structures were true NETs by co-staining Sytox-positive DNA using mAbs directed against MPO and histone H3 citrullination (Figure 5E). Taken together, these data provide evidence that both human and murine hookworm larvae can evade NET-mediated killing through the secretion of a DNase II.

DISCUSSION

The evolution of strategies to overcome trapping by NETs has previously been reported for bacteria, viruses, protozoa, and fungi—the most common of these strategies being the production of a DNase I that targets the backbone structure of the NETs (Derré-Bobillot et al., 2013; Guimarães-Costa et al., 2014; Seper et al., 2013; Sumbly et al., 2005; Thammavongsa et al., 2013). The current study demonstrates that NETs directly contribute to the killing of hookworm larvae *in vitro* and limit parasite viability *in vivo*. We also identified the secretion DNase

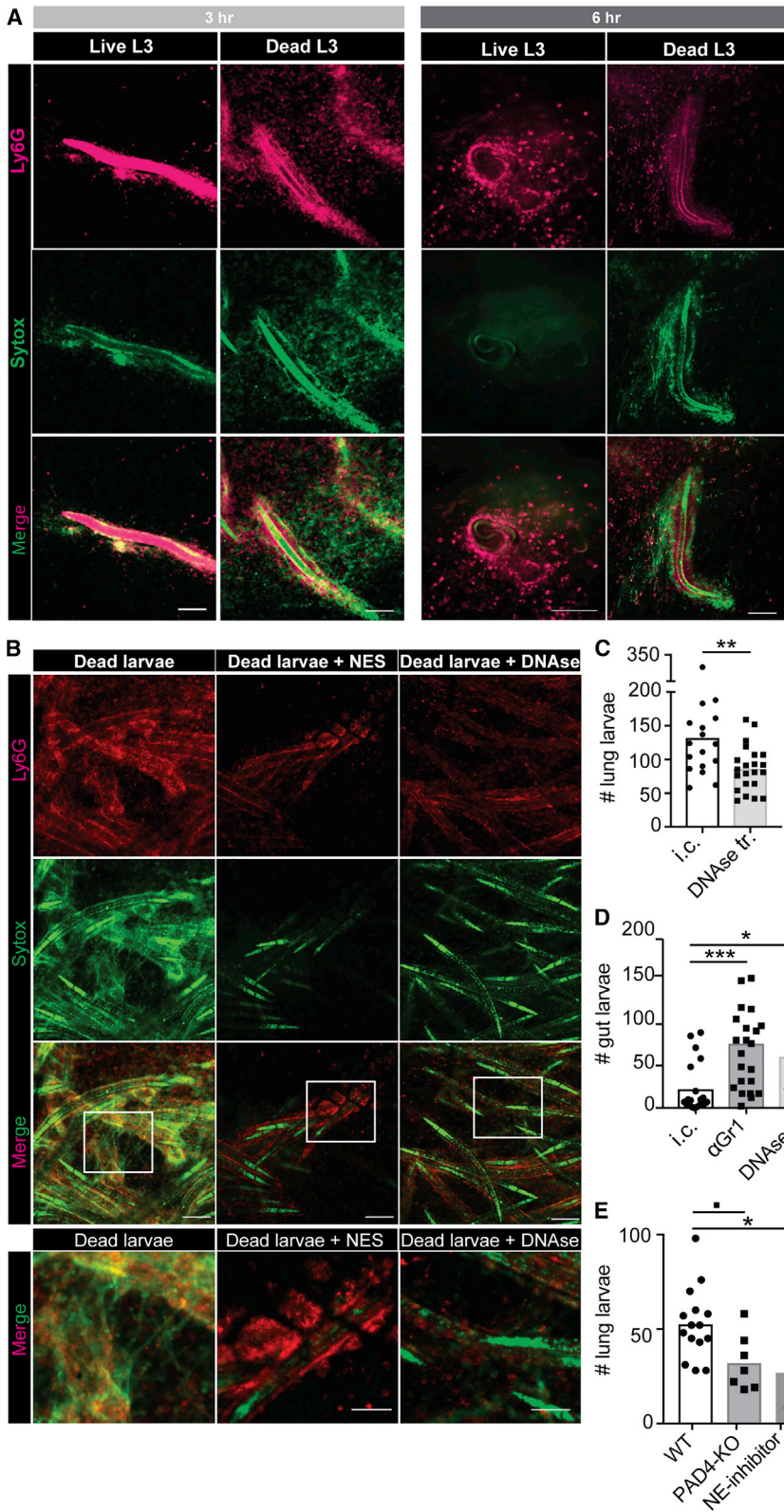


Figure 4. Live Hookworm Larvae, or Their Secreted Products, Can Degrade NETs *In Vivo*

(A and B) Mice were given an i.v. injection of 5 μ g APC-labeled anti-Ly6G mAb and 100 μ L of 50 μ M Sytox-green 1 h before i.d. injection of 250 Nb L3 into the belly skin and infected skin removed 3 or 6 h later and imaged as described in Figure 1A. Images show neutrophils (red) and extracellular DNA (green) and are representative of 2 independent experiments (n = 3 mice/group). Scale bar, 100 μ m. (A) Mice received live or dead (boiled) Nb L3 and the skin imaged 3 or 6 h later. (B) Mice received dead (boiled) Nb L3, with or without 100 μ g of NES, or were additionally given an i.p. injection of 1,000 U of DNase I, and the skin imaged 6 h later.

(C and D) Mice were infected with 250 antibiotic-treated Nb L3 by i.d. injection and additionally treated with 1,000 U of DNase I by i.p. injection at 0, 4, and 8 h post-infection. Worms numbers in the lung at 48 h (C) or gut at 6 days (D). Data are pooled from 2 independent experiments (n = 8–10 mice/group) and analyzed by ANOVA.

€ Wild-type mice were treated with NE-inhibitor by i.p. injection and day -1, 0, and 1. On day 0, wild-type and PAD4-knockout (KO) mice were infected with 250 antibiotic-treated Nb L3 by i.d. injection and the number of larvae in the lung determined at 24 and 48 h. Data are pooled from 2 independent experiments (n = 6–8 mice/group) and analyzed by ANOVA.

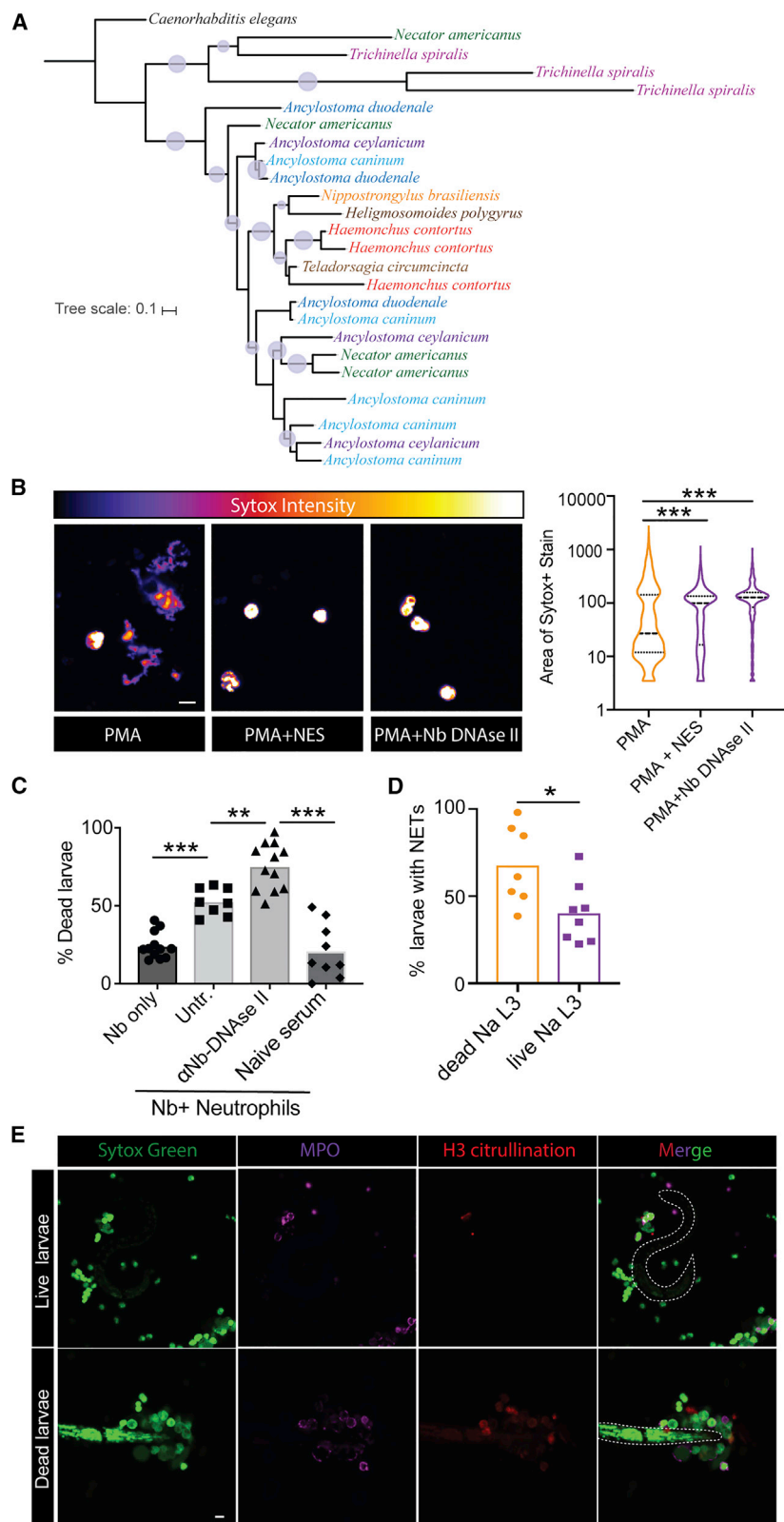


Figure 5. Hookworms Share a Conserved DNase II that Allow Their Evasion from NET-Induced Killing

(A) Phylogenetic relationships of DNase II based on Bayesian inference (BI). The posterior probability supporting each clade is indicated (bootstrap: small circle 0.6, big circle 1).

(B) Human peripheral neutrophils were stimulated with 100 nM PMA to induce NET formation in the presence of 10 μ g/mL of NES. NETs were visualized and their area quantified as described in Figure 3A. More than 1,000 events were recorded for each condition.

(C) 100 Nb L3 were co-cultured with 1 million human peripheral neutrophils for 24 h in presence of antisera raised against Nb-DNase II (α Nb-DNase II, 1:50) or naive serum (1:50). Larvae cultured in the absence of neutrophils were included as a baseline control for viability (Nb only). After overnight co-culture, Sytox green was added (1:100) to the wells and viability of the larvae was assessed using fluorescent microscopy. Larvae were considered dead, or to have impaired viability, when staining positive for the dye. Data are pooled from 3 independent experiments with 1 donor and are representative of 2 additional experiments using a second donor. Data are analyzed by ANOVA.

(D) Human peripheral neutrophils were co-cultured with 100 live (pre-activated overnight at 37C) or dead (boiled) Na L3 for 3 h in presence of Sytox green (1:1,000) and human serum. The formation of NETs around larvae was identified using a fluorescent microscope. Data are presented as the percentage of larvae covered with NETs and pooled from 3 experiments ($n = 2-3$ wells/condition) and analyzed by t test.

(E) Larvae cultured as in (D) were PFA fixed and stained as in Figure 3B. Representative images are shown from 2 experiments (duplicate wells/condition).

II by hookworm larvae as an immunoevasion mechanism employed by the parasite to evade NET-mediated killing.

Bacteria, protozoa, and fungi have all been reported to have evolved strategies to overcome ensnarement by NETs via the secretion of nucleases that degrade the DNA backbone structure of these structures (de Buhr et al., 2014; Jhelum et al., 2018; Sumbly et al., 2005; Zhang et al., 2017). Interestingly, DNase activity has also been described in the excretory and secretory products of various infectious stages of helminths, such as *Trichinella spiralis* and the hookworm *Ancylostoma caninum* (Liu et al., 2007; Yun et al., 2012). In the latter report, the function of the identified DNase activity was not investigated; however, the authors proposed that it may facilitate tissue penetration (Yun et al., 2012). 27 DNase II enzymes have been identified in *Trichinella spiralis* but were reported to miss the DSKW motif, necessary for DNase II enzymatic activity. Our work identifies another function of parasite-secreted DNase, namely the degradation of NETs and evasion of NET-mediated larval killing. It is intriguing that a DNase II, rather than a DNase I, would be secreted by a pathogen. Indeed, the secretion of a DNase II by hookworm larvae was unexpected given that these enzymes are normally restricted to the cytoplasm of all other species investigated to date.

Several recent reports have described the ability of neutrophils contributing to the killing of various nematode larvae (Bonne-Année et al., 2014; McCoy et al., 2017; Pionnier et al., 2016; Sutherland et al., 2014; Tamarozzi et al., 2016). Yet, whether NETs contribute to this killing has remained unclear with some reports describing an association between NETs and the presence of *Strongyloides stercoralis* larvae (Bonne-Année et al., 2014) or microfilariae (Tamarozzi et al., 2016), while others report the presence of neutrophils but not NETs around Nb larvae (Sutherland et al., 2014) and *Brugia malayi* (McCoy et al., 2017). The finding that Nb secretes a DNase II that makes the detection of NETs following natural infection difficult may explain these inconsistencies. Alternatively, different nematode species may exhibit differential abilities to either induce or degrade NETs. In those studies where NETs were reported to surround nematode larvae (Bonne-Année et al., 2014; McCoy et al., 2017; Pionnier et al., 2016; Sutherland et al., 2014; Tamarozzi et al., 2016), it was hypothesized that NETs would not impact on helminth viability directly but that they may instead act to ensnare motile larvae, and thus facilitate their killing by other immune cells (Bonne-Année et al., 2014). Indeed, *S. stercoralis* larvae were reported to be efficiently trapped by NETs, and to be subsequently killed by monocytes (Bonne-Année et al., 2014). Although other cells may well contribute to the killing of hookworm larvae *in vivo*, we provide evidence that NETs alone can directly kill hookworms *in vitro*.

To date, pathogen killing by NETs has been demonstrated for gram-negative and gram-positive bacteria, as well as fungi (Brinkmann et al., 2004; Yipp and Kubes, 2013). Two distinct mechanisms of NET-mediated toxicity have been described. In the first, NETs mediate direct toxicity to bacterial outer membranes via their DNA backbone (Brinkmann and Zychlinsky, 2012; Halverson et al., 2015; Marsman et al., 2016). In the second, killing of fungal pathogens, such as *Candida* and *Aspergillus*, has been shown to be mediated by anti-microbials that

decorate the DNA backbone of NETs (Parker et al., 2012; Urban et al., 2009). Of note, it has been recently been demonstrated that the proteins found within the structure of NETs differ depending on the stimulus used to induce NETosis (Chapman et al., 2019; Lim et al., 2018; Petretto et al., 2019). It would therefore be interesting to elucidate the means by which NETs are toxic to nematode larvae and, if relevant, to identify the proteins that are associated with NETs released in response to these parasites.

How neutrophils are attracted to nematode larvae and what triggers NETosis remains unclear. It has previously been suggested that C5a might be important for recruitment (Giacomin et al., 2008), however, addition of serum was not found to be required *in vitro* to trigger neutrophil chemotaxis toward Nb L3. Rather, our data indicate the neutrophils can respond to larvae directly. However, it is not clear whether neutrophils recognized Nb larvae *per se* or whether they detect bacteria associated with the parasite. Indeed, for *B. malayi*, the symbiont bacterium *Wolbachia* has been shown to be required to trigger NETosis (Tamarozzi et al., 2016). For soil-transmitted helminths like hookworm, bacterial contamination of larvae is common, both in nature and in the laboratory, as L3s emerge from eggs passed out in the feces of infected animals. Given that NETosis in response to nematodes has only been described for soil-transmitted helminths or by filariae containing an endosymbiont bacteria, it is likely that bacterial association is important to this mechanism (Bonne-Année et al., 2014; McCoy et al., 2017; Pionnier et al., 2016; Sutherland et al., 2014; Tamarozzi et al., 2016). In our own experiments, we utilized larvae that were first washed extensively with an antibiotic cocktail, however, residual contamination of bacteria and/or their products is likely making it impossible to distinguish between these possibilities.

Hookworm vaccines currently in development target the adult stage of the parasite, with the lead candidate, Aspartic protease-1 (APR-1), being involved in the ability of the parasite to feed on host blood. While it decreases adult worm survival and associated egg release, it fails to confer sterilizing immunity (Zhan et al., 2014). Here, we show that NETosis can affect both establishment and survival of Nb, despite the fact that the parasite evades the bulk of the immune-mediated attack. Furthermore, the human hookworm Na expresses a homolog of Nb-DNase II that confers the parasite with an evasion strategy. Thus, a useful vaccination approach could be to target the hookworm DNase, in combination with APR-1. This would allow the host to target both larval and adult stages of the parasite and could represent an efficient strategy to both alleviate the pathology induced by the parasite and to decrease the likelihood of establishment and subsequent transmission.

In summary, our findings unveil the ability of NETs to trap and kill infective hookworm larvae in the skin and identify hookworm production of a DNase II as an immune-evasion mechanism employed by these insidious parasites. These findings expand our understanding of mammalian-helminth interactions and open avenues for the development of a successful anti-helminth vaccine, as well as a potential intervention drug for NET-mediated diseases, such as sterile injury, gallstones, septic shock, and autoimmunity.

STAR★METHODS

Detailed methods are provided in the online version of this paper and include the following:

- [KEY RESOURCES TABLE](#)
- [LEAD CONTACT AND MATERIALS AVAILABILITY](#)
- [EXPERIMENTAL MODEL AND SUBJECT DETAILS](#)
 - Mice
 - Preparation and Isolation of *N. brasiliensis* Larvae
 - Isolation of Neutrophils or Monocytes
- [METHOD DETAILS](#)
 - *In Vitro* Co-culture of Neutrophils or Monocytes and Larvae
 - L3 NES Preparation
 - *In Vivo* Treatment
 - Dye Labeling of Live Parasites
 - *Ex Vivo* Imaging of Infected Skin by Laser Scanning Confocal Microscopy
 - Whole Mount Imaging of Infected Skin by Confocal Microscopy
 - *In Vitro* NETosis Imaging and Analysis
 - NET Formation and Lifetime Assays
 - NES Endonuclease Activity Assay
 - Monocyte Viability Assay
 - Protein Selection, RNA Extraction and cDNA Synthesis
 - Gene Cloning
- [QUANTIFICATION AND STATISTICAL ANALYSIS](#)
- [DATA AND CODE AVAILABILITY](#)

SUPPLEMENTAL INFORMATION

Supplemental Information can be found online at <https://doi.org/10.1016/j.chom.2020.01.011>.

ACKNOWLEDGMENTS

We thank the MICU animal facility at Monash AMREP and the Monash Micro Imaging platform for support with confocal imaging. We thank the École Polytechnique Fédérale de Lausanne (EPFL) animal facility, and Jessica Sordet-Dessimoz and EPFL Histology Core Facility, for providing invaluable help and useful suggestions for the experiments outlined. A special thanks to Jose Artacho from the Bio-Imaging and Optics Platform. We also thank the Malaghan BRU for animal husbandry and the Hugh Green Cytometry Centre for help with the microscopy. This work was supported by the Swiss National Science Foundation (SNF310030_156517), the Health Research Council of New Zealand, and the Marjorie Barclay Trust, New Zealand. N.L.H. is supported by a National Health and Medical Research Council (NHMRC) of Australia SRF-B fellowship.

AUTHOR CONTRIBUTIONS

T.B., N.L.H., V.P., and G.L.G. conceived of the idea and participated in the writing of the paper. T.B., M.M., B.V., K.S., M.C., M.K., and G.C. performed infection experiments. T.B. and M.K. prepared the ES of the parasite. T.B., B.V., A. Seitz, and A. Schmidt performed imaging experiments. J.S. and A.L. prepared the recombinant DNase II and performed bioinformatic analyses. T.-D.T., T.B., and S.S. performed *in vitro* assays assessing the deoxyribonuclease activity of NES. T.B. and S.S. performed experiments with Na larvae. G.C. and M.M. proofread the manuscript. All authors discussed the results and commented on the paper.

DECLARATION OF INTERESTS

A.L. and P.G. are shareholders in Paragen Bio Pty Ltd, a biotechnology company focusing on the use of hookworm proteins to treat inflammation.

Received: October 29, 2019
 Revised: December 15, 2019
 Accepted: January 17, 2020
 Published: February 12, 2020

REFERENCES

- Aga, E., Katschinski, D.M., van Zandbergen, G., Laufs, H., Hansen, B., Müller, K., Solbach, W., and Laskay, T. (2002). Inhibition of the spontaneous apoptosis of neutrophil granulocytes by the intracellular parasite *Leishmania major*. *J. Immunol.* **169**, 898–905.
- Allen, J.E., and Maizels, R.M. (2011). Diversity and dialogue in immunity to helminths. *Nat. Rev. Immunol.* **11**, 375–388.
- Anthony, R.M., Rutitzky, L.I., Urban, J.F., Jr., Stadecker, M.J., and Gause, W.C. (2007). Protective immune mechanisms in helminth infection. *Nat. Rev. Immunol.* **7**, 975–987.
- Araújo, A., Ferreira, L.F., Confalonieri, U., and Chame, M. (1988). Hookworms and the peopling of America. *Cad. Saude Publica* **4**, 226–233.
- Bonne-Année, S., Kerepesi, L.A., Hess, J.A., Wesolowski, J., Paumet, F., Lok, J.B., Nolan, T.J., and Abraham, D. (2014). Extracellular traps are associated with human and mouse neutrophil and macrophage mediated killing of larval *Strongyloides stercoralis*. *Microbes Infect.* **16**, 502–511.
- Bouchery, T., Kyle, R., Camberis, M., Shepherd, A., Filbey, K., Smith, A., Harvie, M., Painter, G., Johnston, K., Ferguson, P., et al. (2015). ILC2s and T cells cooperate to ensure maintenance of M2 macrophages for lung immunity against hookworms. *Nat. Commun.* **6**, 6970.
- Branzk, N., Lubojemska, A., Hardison, S.E., Wang, Q., Gutierrez, M.G., Brown, G.D., and Papayannopoulos, V. (2014). Neutrophils sense microbe size and selectively release neutrophil extracellular traps in response to large pathogens. *Nat. Immunol.* **15**, 1017–1025.
- Brinkmann, V., Reichard, U., Goosmann, C., Fauler, B., Uhlemann, Y., Weiss, D.S., Weinrauch, Y., and Zychlinsky, A. (2004). Neutrophil extracellular traps kill bacteria. *Science* **303**, 1532–1535.
- Brinkmann, V., and Zychlinsky, A. (2012). Neutrophil extracellular traps: is immunity the second function of chromatin? *J. Cell Biol.* **198**, 773–783.
- Byrd, A.S., O'Brien, X.M., Johnson, C.M., Lavigne, L.M., and Reichner, J.S. (2013). An extracellular matrix-based mechanism of rapid neutrophil extracellular trap formation in response to *Candida albicans*. *J. Immunol.* **190**, 4136–4148.
- Camberis, M., Le Gros, G., and Urban, J., Jr. (2003). Animal model of *Nippostrongylus brasiliensis* and *Heligmosomoides polygyrus*. *Curr Protoc Immunol.* **55**, <https://doi.org/10.1002/0471142735.im1912s55>.
- Chapman, E.A., Lyon, M., Simpson, D., Mason, D., Beynon, R.J., Moots, R.J., and Wright, H.L. (2019). Caught in a Trap? Proteomic Analysis of Neutrophil Extracellular Traps in Rheumatoid Arthritis and Systemic Lupus Erythematosus. *Front. Immunol.* **10**, 423.
- Chen, F., Wu, W., Millman, A., Craft, J.F., Chen, E., Patel, N., Boucher, J.L., Urban, J.F., Jr., Kim, C.C., and Gause, W.C. (2014). Neutrophils prime a long-lived effector macrophage phenotype that mediates accelerated helminth expulsion. *Nat. Immunol.* **15**, 938–946.
- Datu, B.J., Gasser, R.B., Nagaraj, S.H., Ong, E.K., O'Donoghue, P., McInnes, R., Ranganathan, S., and Loukas, A. (2008). Transcriptional changes in the hookworm, *Ancylostoma caninum*, during the transition from a free-living to a parasitic larva. *PLoS Negl. Trop. Dis.* **2**, e130.
- de Buhr, N., Neumann, A., Jerjomiceva, N., von Köckritz-Blickwede, M., and Baums, C.G. (2014). *Streptococcus suis* DNase SsnA contributes to degradation of neutrophil extracellular traps (NETs) and evasion of NET-mediated antimicrobial activity. *Microbiology* **160**, 385–395.
- Derré-Bobillot, A., Cortes-Perez, N.G., Yamamoto, Y., Kharrat, P., Couvé, E., Da Cunha, V., Decker, P., Boissier, M.C., Escartin, F., Cesselin, B., et al. (2013).

- Nuclease A (Gbs0661), an extracellular nuclease of *Streptococcus agalactiae*, attacks the neutrophil extracellular traps and is needed for full virulence. *Mol. Microbiol.* 89, 518–531.
- Díaz-Godínez, C., and Carrero, J.C. (2019). The state of art of neutrophil extracellular traps in protozoan and helminthic infections. *Biosci. Rep.* 39, BSR20180916.
- Edgar, R.C. (2004). MUSCLE: multiple sequence alignment with high accuracy and high throughput. *Nucleic Acids Res.* 32, 1792–1797.
- Epp, J.R., Niibori, Y., Liz Hsiang, H.L., Mercaldo, V., Deisseroth, K., Josselyn, S.A., and Frankland, P.W. (2015). Optimization of CLARITY for Clearing Whole-Brain and Other Intact Organs(1,2,3). *eNeuro* 2, ENEURO.0022-15.2015.
- Finn, R.D., Clements, J., and Eddy, S.R. (2011). HMMER web server: interactive sequence similarity searching. *Nucleic Acids Res.* 39, W29–37.
- Giacomin, P.R., Gordon, D.L., Botto, M., Daha, M.R., Sanderson, S.D., Taylor, S.M., and Dent, L.A. (2008). The role of complement in innate, adaptive and eosinophil-dependent immunity to the nematode *Nippostrongylus brasiliensis*. *Mol. Immunol.* 45, 446–455.
- Guimarães-Costa, A.B., DeSouza-Vieira, T.S., Paletta-Silva, R., Freitas-Mesquita, A.L., Meyer-Fernandes, J.R., and Saraiva, E.M. (2014). 3'-nucleotidase/nuclease activity allows *Leishmania* parasites to escape killing by neutrophil extracellular traps. *Infect. Immun.* 82, 1732–1740.
- Guindon, S., Dufayard, J.F., Lefort, V., Anisimova, M., Hordijk, W., and Gascuel, O. (2010). New algorithms and methods to estimate maximum-likelihood phylogenies: assessing the performance of PhyML 3.0. *Syst. Biol.* 59, 307–321.
- Halverson, T.W., Wilton, M., Poon, K.K., Petri, B., and Lewenza, S. (2015). DNA is an antimicrobial component of neutrophil extracellular traps. *PLoS Pathog.* 11, e1004593.
- Hawdon, J.M., and Schad, G.A. (1990). Serum-stimulated feeding in vitro by third-stage infective larvae of the canine hookworm *Ancylostoma caninum*. *J. Parasitol.* 76, 394–398.
- Hotez, P.J. (2008). Tropical diseases research: thirty years and counting. *PLoS Negl. Trop. Dis.* 2, e329.
- Hotez, P.J., Beaumier, C.M., Gillespie, P.M., Strych, U., Hayward, T., and Bottazzi, M.E. (2016). Advancing a vaccine to prevent hookworm disease and anemia. *Vaccine* 34, 3001–3005.
- Hotez, P.J., and Pecoul, B. (2010). “Manifesto” for advancing the control and elimination of neglected tropical diseases. *PLoS Negl. Trop. Dis.* 4, e718.
- Jhelum, H., Sori, H., and Sehgal, D. (2018). A novel extracellular vesicle-associated endodeoxyribonuclease helps *Streptococcus pneumoniae* evade neutrophil extracellular traps and is required for full virulence. *Sci. Rep.* 8, 7985.
- Knott, M.L., Matthaie, K.I., Giacomin, P.R., Wang, H., Foster, P.S., and Dent, L.A. (2007). Impaired resistance in early secondary *Nippostrongylus brasiliensis* infections in mice with defective eosinophilopoiesis. *Int. J. Parasitol.* 37, 1367–1378.
- Letunic, I., and Bork, P. (2019). Interactive Tree Of Life (iTOL) v4: recent updates and new developments. *Nucleic Acids Res.* 47 (W1), W256–W259.
- Lim, C.H., Adav, S.S., Sze, S.K., Choong, Y.K., Saravanan, R., and Schmidtchen, A. (2018). Thrombin and Plasmin Alter the Proteome of Neutrophil Extracellular Traps. *Front. Immunol.* 9, 1554.
- Liu, M.Y., Wang, X.L., Fu, B.Q., Li, C.Y., Wu, X.P., Le Rhun, D., Chen, Q.J., and Boireau, P. (2007). Identification of stage-specifically expressed genes of *Trichinella spiralis* by suppression subtractive hybridization. *Parasitology* 134, 1443–1455.
- Marsman, G., Zeerleder, S., and Luken, B.M. (2016). Extracellular histones, cell-free DNA, or nucleosomes: differences in immunostimulation. *Cell Death Dis.* 7, e2518.
- McCoy, C.J., Reaves, B.J., Giguère, S., Coates, R., Rada, B., and Wolstenholme, A.J. (2017). Human Leukocytes Kill *Brugia malayi* Microfilariae Independently of DNA-Based Extracellular Trap Release. *PLoS Negl. Trop. Dis.* 11, e0005279.
- McDonald, B., Urrutia, R., Yipp, B.G., Jenne, C.N., and Kubes, P. (2012). Intravascular neutrophil extracellular traps capture bacteria from the bloodstream during sepsis. *Cell Host Microbe* 12, 324–333.
- Mendez, J., Sun, D., Tuo, W., and Xiao, Z. (2018). Bovine neutrophils form extracellular traps in response to the gastrointestinal parasite *Ostertagia ostertagi*. *Sci. Rep.* 8, 17598.
- Muñoz-Caro, T., Mena Huertas, S.J., Conejeros, I., Alarcón, P., Hidalgo, M.A., Burgos, R.A., Hermosilla, C., and Taubert, A. (2015). Eimeria bovis-triggered neutrophil extracellular trap formation is CD11b-, ERK 1/2-, p38 MAP kinase- and SOCE-dependent. *Vet. Res. (Faisalabad)* 46, 23.
- Neubert, E., Meyer, D., Rocca, F., Günay, G., Kwaczala-Tessmann, A., Grandke, J., Senger-Sander, S., Geisler, C., Egner, A., Schön, M.P., et al. (2018). Chromatin swelling drives neutrophil extracellular trap release. *Nat. Commun.* 9, 1–13, <https://doi.org/10.1038/s41467-018-06263-5>.
- Obata-Ninomiya, K., Ishiwata, K., Tsutsui, H., Nei, Y., Yoshikawa, S., Kawano, Y., Minegishi, Y., Ohta, N., Watanabe, N., Kanuka, H., and Karasuyama, H. (2013). The skin is an important bulwark of acquired immunity against intestinal helminths. *J. Exp. Med.* 210, 2583–2595.
- Papayannopoulos, V. (2014). Infection: microbial nucleases turn immune cells against each other. *Curr. Biol.* 24, R123–R125.
- Parker, H., Albrett, A.M., Kettle, A.J., and Winterbourn, C.C. (2012). Myeloperoxidase associated with neutrophil extracellular traps is active and mediates bacterial killing in the presence of hydrogen peroxide. *J. Leukoc. Biol.* 91, 369–376.
- Pellegrines, C., Tang, S.C., Schmidt, A., White, R.F., Lamiabile, O., Connor, L.M., Ruedl, C., Dobrucki, J., Le Gros, G., and Ronchese, F. (2017). Toll-Like Receptor 4, but Not Neutrophil Extracellular Traps, Promote IFN Type I Expression to Enhance Th2 Responses to *Nippostrongylus brasiliensis*. *Front. Immunol.* 8, 1575.
- Petersen, T.N., Brunak, S., von Heijne, G., and Nielsen, H. (2011). SignalP 4.0: discriminating signal peptides from transmembrane regions. *Nat. Methods* 8, 785–786.
- Petretto, A., Bruschi, M., Pratesi, F., Croia, C., Candiano, G., Ghiggeri, G., and Migliorini, P. (2019). Neutrophil extracellular traps (NET) induced by different stimuli: A comparative proteomic analysis. *PLoS One* 14, e0218946.
- Pionnier, N., Brotin, E., Karadjian, G., Hemon, P., Gaudin-Nomé, F., Vallarino-Lhermitte, N., Nieguitsila, A., Fercocq, F., Akrin, M.L., Marin-Esteban, V., et al. (2016). Neutropenic Mice Provide Insight into the Role of Skin-Infiltrating Neutrophils in the Host Protective Immunity against Filarial Infective Larvae. *PLoS Negl. Trop. Dis.* 10, e0004605.
- Rogers, W.P., and Sommerville, R.I. (1957). Physiology of exsheathment in nematodes and its relation to parasitism. *Nature* 179, 619–621.
- Saitoh, T., Komano, J., Saitoh, Y., Misawa, T., Takahama, M., Kozaki, T., Uehata, T., Iwasaki, H., Omori, H., Yamaoka, S., et al. (2012). Neutrophil extracellular traps mediate a host defense response to human immunodeficiency virus-1. *Cell Host Microbe* 12, 109–116.
- Schindelin, J., Arganda-Carreras, I., Frise, E., Kaynig, V., Longair, M., Pietzsch, T., Preibisch, S., Rueden, C., Saalfeld, S., Schmid, B., et al. (2012). Fiji: an open-source platform for biological-image analysis. *Nat. Methods* 9, 676–682.
- Seper, A., Hosseinzadeh, A., Gorkiewicz, G., Lichtenegger, S., Roier, S., Leitner, D.R., Röhm, M., Grutsch, A., Reidl, J., Urban, C.F., and Schild, S. (2013). *Vibrio cholerae* evades neutrophil extracellular traps by the activity of two extracellular nucleases. *PLoS Pathog.* 9, e1003614.
- Sotillo, J., Sanchez-Flores, A., Cantacessi, C., Harcus, Y., Pickering, D., Bouchery, T., Camberis, M., Tang, S.C., Giacomin, P., Mulvenna, J., et al. (2014). Secreted proteomes of different developmental stages of the gastrointestinal nematode *Nippostrongylus brasiliensis*. *Mol. Cell. Proteomics* 13, 2736–2751.
- Sumby, P., Barbian, K.D., Gardner, D.J., Whitney, A.R., Welty, D.M., Long, R.D., Bailey, J.R., Parnell, M.J., Hoe, N.P., Adams, G.G., et al. (2005). Extracellular deoxyribonuclease made by group A *Streptococcus* assists pathogenesis by enhancing evasion of the innate immune response. *Proc. Natl. Acad. Sci. USA* 102, 1679–1684.

- Sutherland, T.E., Logan, N., Rückerl, D., Humbles, A.A., Allan, S.M., Papayannopoulos, V., Stockinger, B., Maizels, R.M., and Allen, J.E. (2014). Chitinase-like proteins promote IL-17-mediated neutrophilia in a tradeoff between nematode killing and host damage. *Nat. Immunol.* **15**, 1116–1125.
- Tamarozzi, F., Turner, J.D., Pionnier, N., Midgley, A., Guimaraes, A.F., Johnston, K.L., Edwards, S.W., and Taylor, M.J. (2016). *Wolbachia* endosymbionts induce neutrophil extracellular trap formation in human onchocerciasis. *Sci. Rep.* **6**, 35559.
- Tang, Y.T., Gao, X., Rosa, B.A., Abubucker, S., Hallsworth-Pepin, K., Martin, J., Tyagi, R., Heizer, E., Zhang, X., Bhonagiri-Palsikar, V., et al. (2014). Genome of the human hookworm *Necator americanus*. *Nat. Genet.* **46**, 261–269.
- Thammavongsa, V., Missiakas, D.M., and Schneewind, O. (2013). *Staphylococcus aureus* degrades neutrophil extracellular traps to promote immune cell death. *Science* **342**, 863–866.
- Urban, C.F., Ermert, D., Schmid, M., Abu-Abed, U., Goosmann, C., Nacken, W., Brinkmann, V., Jungblut, P.R., and Zychlinsky, A. (2009). Neutrophil extracellular traps contain calprotectin, a cytosolic protein complex involved in host defense against *Candida albicans*. *PLoS Pathog.* **5**, e1000639.
- Urban, C.F., Reichard, U., Brinkmann, V., and Zychlinsky, A. (2006). Neutrophil extracellular traps capture and kill *Candida albicans* yeast and hyphal forms. *Cell. Microbiol.* **8**, 668–676.
- Walker, I.H., Hsieh, P.C., and Riggs, P.D. (2010). Mutations in maltose-binding protein that alter affinity and solubility properties. *Appl. Microbiol. Biotechnol.* **88**, 187–197.
- Weinstein, P.P., and Jones, M.F. (1956). The in vitro cultivation of *Nippostrongylus muris* to the adult stage. *J. Parasitol.* **42**, 215–236.
- Yanagihara, K., Fukuda, Y., Seki, M., Izumikawa, K., Miyazaki, Y., Hirakata, Y., Tsukamoto, K., Yamada, Y., Kamhira, S., and Kohno, S. (2007). Effects of specific neutrophil elastase inhibitor, sivelestat sodium hydrate, in murine model of severe pneumococcal pneumonia. *Exp. Lung Res.* **33**, 71–80.
- Yipp, B.G., and Kuberski, P. (2013). NETosis: how vital is it? *Blood* **122**, 2784–2794.
- Yipp, B.G., Petri, B., Salina, D., Jenne, C.N., Scott, B.N., Zbytniuk, L.D., Pittman, K., Asaduzzaman, M., Wu, K., Meijndert, H.C., et al. (2012). Infection-induced NETosis is a dynamic process involving neutrophil multi-tasking in vivo. *Nat. Med.* **18**, 1386–1393.
- Yun, S.H., Seo, M.G., Jung, B.Y., Kim, T.H., Kwon, O.D., Jeong, K.S., Rhee, M.H., Lee, Y.J., Park, S.J., Kwon, Y.S., and Kwak, D. (2012). Characteristics of DNase activities in excretory/secretory products of infective larvae of *Haemonchus contortus*. *J. Helminthol.* **86**, 363–367.
- Zhan, B., Beaumier, C.M., Briggs, N., Jones, K.M., Keegan, B.P., Bottazzi, M.E., and Hotez, P.J. (2014). Advancing a multivalent 'Pan-anthelmintic' vaccine against soil-transmitted nematode infections. *Expert Rev. Vaccines* **13**, 321–331.
- Zhang, X., Zhao, S., Sun, L., Li, W., Wei, Q., Ashman, R.B., and Hu, Y. (2017). Different virulence of *Candida albicans* is attributed to the ability of escape from neutrophil extracellular traps by secretion of DNase. *Am. J. Transl. Res.* **9**, 50–62.

STAR★METHODS

KEY RESOURCES TABLE

REAGENT or RESOURCE	SOURCE	IDENTIFIER
Antibodies		
Human/Mouse anti-Myeloperoxidase	R&D system	Cat#AF3667; RRID:AB_2250866
Rabbit polyclonal to Histone H3 (citrulline R2 + R8 + R17)	Abcam	Cat#ab5103; RRID:AB_304752
anti-Gr1, clone RB6-8C5 (depletion)	BioXcell	Cat#BE0075; RRID:AB_10312146
Anti-Ly6G, clone 1A8 (depletion)	BioXcell	Cat#BE0075-1; RRID:AB_1107721
InVivoMAb rat IgG2a isotype control, clone 2A3 (depletion)	BioXcell	Cat#BE0089; RRID:AB_1107769
InVivoPlus rat IgG2b isotype control, clone LTF-2	BioXcell	Cat#BE0090; RRID:AB_1107780
BV421 anti-Ly6G, clone AL-21 (<i>in vivo</i> staining)	BD	Cat#562727; RRID:AB_2737748
AlexaFluor 647 anti-Gr1, clone RB6-8C5 (<i>in vivo</i> staining)	Biolegend	Cat#108420; RRID:AB_493481
AlexaFluor 647 anti-Ly6G, clone 1A8 (<i>in vivo</i> staining)	BD	Cat#127609; RRID:AB_1134162
Bacterial and Virus Strains		
<i>E. coli</i> BL21 (DE3)	Thermo-Fisher Scientific	Cat#C600003
Biological Samples		
Nippostrongylus excretory Secretory (NES) products	Camberis et al., 2003	N/A
Mouse polyclonal serum anti-NES	This paper	N/A
Chemicals, Peptides, and Recombinant Proteins		
DNase I, bovine recombinant	Sigma-Aldrich (Roche)	Cat#04536282001
Sytox green nucleic ac	Life technologies	Cat#S7020
Sytox blue nucleic acid	Life technologies	Cat#S11348
Phorbol 12-myristate 13-acetate	Sigma-Aldrich	Cat#79346-1MG
NE-inhibitor, sivelestat sodium hydrate	Sigma-Aldrich	Cat#S7198-5MG
Carboxyl fluorescein succinimidyl ester	Sigma-Aldrich	Cat#92846-5MG-F
Fluorobrite YO carboxylate microsphere	Polysciences, Inc	Cat#18720-10
Fluorobrite	Thermo-fisher	Cat#A1896701
CUBIC mount	Epp et al., 2015	N/A
Critical Commercial Assays		
MACS Neutrophil Isolation Kit, mouse	Miltenyi Biotec	Cat#130-097-658
Lympholyte-Poly	Cedarlane	Cat#CL5070
Deposited Data		
Fiji Macro for measuring distance of cells to a an helminth parasite	This paper	10.5281/zenodo.3596520
Nb_DNase_II	This paper	GenBank: M938457
Experimental Models: Organisms/Strains		
<i>Nippostrongylus brasiliensis</i>	Monash University - original strain Laboratory of Lindsay Dent	N/A
<i>Necator americanus</i>	JICU	N/A
Mouse: C57BL/6	Charles River	N/A
Mouse: C57BL/6	Monash University	N/A
Mouse: C57BL/6	EPFL	N/A
Mouse: PAD4-KO (C57BL/6 background)	The Francis Crick Institute	N/A
Candida albicans	SC5314 clinical isolate (The Francis Crick Institute)	N/A

(Continued on next page)

Continued

REAGENT or RESOURCE	SOURCE	IDENTIFIER
Oligonucleotides		
Forward primer for NB-DNase II: Nb-m.13872F (5'-GCG CATATGGAATTCGGTCTGAGTTGCAAGAACATG-3')	This paper	N/A
Reverse primer for NB-DNase II: Nb-m.13872R (5'-CGCCTCGAGGCGGTTTTGTTGTCTTCTT-3')	This paper	N/A
Recombinant DNA		
pMAL-c2X plasmid	Walker et al., 2010	Addgene Cat#75286
Software and Algorithms		
Fiji	Schindelin et al., 2012	https://imagej.nih.gov/ij/
HMMERv3.2	Finn et al., 2011	N/A
SignalP v4.0	Petersen et al., 2011	http://www.cbs.dtu.dk/services/SignalP/
MUSCLE	Edgar, 2004	http://www.drive5.com/muscle/downloads.htm
PhyML	Guindon et al., 2010	http://www.atgc-montpellier.fr/phyml/
The Interactive Tree of Life (iTOF)	Letunic and Bork, 2019	https://itol.embl.de/
GraphPad Prism 8		https://www.graphpad.com/scientific-software/prism/
Minitab 17 Statistical Software		www.minitab.com
Other		
μ -Slide 8 Well ibiTreat	Ibidi	Cat#80826

LEAD CONTACT AND MATERIALS AVAILABILITY

Further information and requests for resources and reagents should be directed to and will be fulfilled by the Lead Contact, Prof. Nicola Harris (nicola.harris@monash.edu).

Requests for the plasmid encoding the recombinant Nb-DNase II generated in this study should be made to Prof. Nicola Harris and Prof. Alex Loukas (alex.loukas@jcu.edu.au). Note that it will be made available on request but we may require a completed Materials Transfer Agreement if there is potential for commercial application.

EXPERIMENTAL MODEL AND SUBJECT DETAILS**Mice**

C57BL/6J (WT) mice were obtained from Charles River Laboratories. All mice were maintained under specific pathogen-free (SPF) conditions at École Polytechnique Fédérale de Lausanne (EPFL), Switzerland or by the Monash Intensive Care Unit Facility at Monash University, AMREP campus Melbourne, Australia or by the Biomedical Research Unit, Malaghan Institute of Medical Research, Wellington, New Zealand. PAD4-KO mice were maintained at the Francis Crick institute. All mice were age and sex-matched and used between 6-14 weeks of age. Littermates of the same sex were randomly assigned to experimental groups. Mice were maintained at 3-5 animal per cage and ad libitum access to water and food. All animal experiments were approved by the Service de la consommation et des affaires vétérinaires (1066 Épalinges, Canton of Vaud, Switzerland) with the authorization number VD 3001, or by the AEC committee of the Alfred campus, Melbourne Australia with authorization number E/1846/2018/M or by the Victoria University of Wellington, Wellington, New Zealand.

Preparation and Isolation of *N. brasiliensis* Larvae

Nb was maintained by monthly passage in Lewis rats. Infective larvae (L3) were prepared from 2 week old rat fecal cultures as previously described (Camberis et al., 2003). Prior to infection, larvae were washed in a mix of (Penicillin/Streptomycin 1000 U/mL (GIBCO), Gentamicin 300 U/mL (Sigma) in PBS), for 30 min and then rinsed in sterile PBS. 250 L3 were delivered by id. injection in 10 μ L of sterile PBS to the belly skin. Of note, because of the low volume for infection, the dose of infection is more variable than what is classically expected for this parasite. For injection into the belly skin, mice were prepared one day earlier by removing a small area of hair from the injection site using tweezers.

Isolation of Neutrophils or Monocytes**Mouse**

Neutrophils and monocytes were isolated from the mouse bone marrow of naive mice using negative selection MACS separation kits.

Human

Neutrophils were isolated from fresh blood of healthy donors (the sex is unknown) using Lympholyte-Poly, as recommended by the manufacturer.

Cells were plated at 1 million per well in a 24 well plate and cultured 10% FBS, RPMI at 37°C, 5% CO₂. Purity was assessed by cytoSpin followed by a Diff-quick stain.

For experiments that took place in EPFL (Switzerland), the samples were provided via the blood center of the *Transfusion Interregionale CRS* (Epalinges, Switzerland) in accordance with the Cantonal Ethics committee of the Canton of Vaud (Vaud Switzerland). Written consent from the donors was obtained by the Lausanne blood transfusion center, the donors agreed that after absolute anonymity that certain components of their blood be used for medical research purposes. For experiments that took place in Monash University (Australia), blood was taken by an authorized person in the department from anonymous donors in agreement with the application CF07/0141-2007/0025, approved by Monash University (Medicine and Dentistry Human Ethics Sub-Committee). Written consent from the donors was obtained prior to drawing blood, and the donors agreed that after absolute anonymity that their blood be used for medical research purposes.

METHOD DETAILS

In Vitro Co-culture of Neutrophils or Monocytes and Larvae

Primary cells were cultured at 1 million per well in a 24 well plate in presence of 100 antibiotic-treated Nb or Necator L3 in complete RPMI. Cellular adherence to the larvae was assessed 24 h later using an inverted bright-field microscope. To measure viability, Sytox Green was added at 1:100 dilution 15 min prior to imaging on a fluorescent inverted microscope.

For chemotaxis assays, neutrophils were placed on the upper chamber formed by a 4 µm pore transwell (Ibidi), while larvae were placed in the lower chamber. The number of neutrophils that migrated from the upper to the lower chamber was assessed after 24 h using an inverted brightfield microscope.

L3 NES Preparation

For the generation of Nb excretory/secretory (NES) products, L3 were washed extensively in sterile PBS supplemented with penicillin and streptomycin, incubated for a further 1 h in RPMI (GIBCO) supplemented with penicillin and streptomycin then cultured at 37°C, 5% CO₂ in RPMI containing antibiotics (penicillin, streptomycin, gentamicin and tetracycline; Sigma-Aldrich) and 1% glucose (Sigma-Aldrich). The supernatant was collected every 2 days for a period of 2 weeks and was subjected to sterile filtration then concentrated by centrifugation through a 10,000 MWCO cellulose membrane (Centriprep; Millipore). Contaminating LPS was removed using an EndoTrap Blue LPS-binding affinity column (Hyglos GmbH, Germany). The concentration of residual endotoxin was determined using the Limulus Assay (Lonza), and only those batches found to contain less than 1 U LPS per 1 µg protein were used for experiments.

In Vivo Treatment

Where indicated anti-Gr1 mAb (RB6-8C5, 0.250mg) or anti-Ly6G mAb (1A8, 0.5 mg) were administered intraperitoneally at day -1, 0 and 1 of infection. Cellular depletion efficiency was evaluated by flow cytometry in the blood and by imaging of the infected skin.

For imaging granulocyte recruitment, anti-Gr1 mAb (RB6-8C5, 10 µg), anti-Ly6G mAb (1A8, 5 µg) or anti-Ly6C mAb (AL-21, 5 µg) were injected intravenously 1 h before infection.

For experiments employing DNase I, mice were treated with 1000 U recombinant DNase I (Roche) intraperitoneally every 4 h for a total of 12 h starting at the time of infection.

For experiments using NES, mice were injected via the intradermal route with 10 µL of 100 µg LPS-depleted NES together with Nb L3.

Dye Labeling of Live Parasites

For external labeling of the larval sheath L3 were washed several times in PBS then incubated at room temperature for 8 min in 2.5 mM carboxyl fluorescein succinimidyl ester (CFSE, Sigma-Aldrich, Ex. 492 nm/Em. 517 nm), and washed in PBS three times prior to use for infection. For internal larval labeling, L3 were sterilized by washing in antibiotics and then fed with Fluorospire YO carboxylate microsphere (Polysciences, Inc, Ex. 529nm/ Em. 546 nm) beads for 4 h. Larvae were then washed in PBS containing 0.05% tween prior to use for infection. The efficiency of staining and the viability of larvae was verified by microscopy prior to infection.

Ex Vivo Imaging of Infected Skin by Laser Scanning Confocal Microscopy

Fluorescence imaging of neutrophils, monocytes and/or NETs was performed using imaging by immunofluorescence microscopy of skin flaps immediately following their removal from sacrificed animals. At the time of necropsy, a skin flap of the site of injection was removed and mounted in complete Fluorospire on a slide with a 1 mm thick holding chamber. The subcutaneous tissue facing upward was covered with a coverslip and placed to image upside down on a heating pad. Images were acquired on Zeiss LSM700 laser scanning confocal microscope mounted in an inverted microscope equipped with 20 × objective, 1.2 N.A. using regular photomultiplier tubes (PMTs), 1-a.u. pinhole. Each image was acquired using the indicated fluorescent channels and the same acquisition settings across different samples.

To control for differences in background fluorescence between experiments and antibody/dye batches, the contrast was adjusted to minimize autofluorescence and a minimum brightness threshold was set such that only positive staining could be visualized. The same contrast and threshold values were applied to all images taken across all treatment groups within a single experiment using Fiji (Schindelin et al., 2012).

For the quantitative analysis of myeloid cell recruitment around larvae, including a measure of their distance from the larvae, a custom-made macro was generated as described in Figure S2. Briefly, in Fiji, the 'Region of Interest' was defined as the outline of the worm. A distance map was defined and binarized signal for each fluorescent dye used to measure the percentage of area of stain depending of the distance to the larvae.

Extracellular DNA was labeled by iv. injection of 100 μ L of Sytox Green (Ex. 504 nm/ Em. 523 nm) or Sytox blue (Ex. 444 nm/ Em. 480 nm) DNA dye (50 μ M). Monocyte and neutrophil recruitment were visualized by iv. injection of AlexaFluor 647-anti-mouse Gr1 antibody (Clone RB6-8C5), AlexaFluor 647-anti-mouse Ly6G antibody (Clone 1A8) and BV421-anti-mouse Ly6C antibody (Clone AL-21). All antibodies and dyes were injected intravenously 1 h prior to infection. For imaging of myeloid cell recruitment following the topical application of larvae, L3 were applied to untreated skin at 40 min intervals for a total of 12 applications. Infected skin was removed and imaged 1 h following the last larval application, and washed extensively with water to remove any remaining external larvae.

Whole Mount Imaging of Infected Skin by Confocal Microscopy

1 cm² of skin around the injection site was removed stretched, with the subcutaneous tissue orientated to face upward, onto a silicon plate and fixed in place using pins. The tissue was fixed overnight in 4% PFA under constant agitation. The next day tissue was rehydrated in 20% sucrose for 24 h. The skin was then soaked in PBS containing 1% donkey serum and 0.05% Triton X-100 for an additional 24 h. Primary antibodies were added to the tissue for 30 min and then centrifuged at 600 g for 6 h at 4°C (to aid penetration of the antibodies into the tissue). Tissue sections were then washed extensively before applying the secondary antibodies, which were also incubated for 30 min and then centrifuged at 600 g for 1.5 h at 4°C. Following another washing step stained tissues were placed in CUBIC (Epp et al., 2015) for at least 48 h to clear the tissue prior to imaging.

Images were acquired using a Zeiss LSM700 laser scanning confocal microscope mounted in an inverted microscope equipped with 20 \times objective, 1.2 N.A. using regular PMTs, 1-a.u. pinhole or Nikon A1r laser scanning confocal microscope mounted on an inverted microscope equipped with 20 \times objective, 1.2 NA using regular PMTs, 1-a.u. pinhole. Each image was acquired using the indicated fluorescent channels and the same acquisition setting across different samples. Images were analyzed using Fiji (Schindelin et al., 2012). The same contrast and threshold values were applied to all images from all treatment groups within a given experiment. For quantification of the area of positive signal relative to the distance to the larvae, a custom-made macro was used as described in the previous section.

In Vitro NETosis Imaging and Analysis

Human neutrophils were isolated using A lympholyte Poly gradient separation (Cedarlane). 50 000 cells were co-cultured with 100 L3 antibiotic treated Nb or Necator larvae in complete RPMI containing 10% serum and 1% penicillin/streptomycin/tetracyclin in a 8 well μ -Slide (Ibidi®). Cells were incubated at 37°C, 5% CO₂ for 1 hr prior to imaging. Just before imaging 1 μ L/well of sytox Blue or Green (5mM) was added to each well. Images were acquired on Zeiss LSM700 laser scanning confocal microscope (20 \times /1.2 using regular photomultiplier tubes (PMTs), pinhole as closed as possible, (i.e., < 1 Airy Unit) laser confocal inverted microscope equipped with a heating chamber. Each image was acquired using the indicated fluorescent channels and the same acquisition setting employed across different samples. Images were analyzed using ImageJ. The same contrast and threshold values were applied to all images from all treatment groups within the experiment. The fire LUT was used to facilitate viewing of the thin filament constitutive of the extracellular traps. Quantification of Area of sytox+ events was made with Fiji using the following analysis workflow: first particles were identified using "Find edges." Then the image was binarized using an automatic thresholding algorithm (Otsu). The particles were then treated using "Dilate" (settings: 2) to avoid the counting of segmented nuclei and to allow easier identification of the thin filamentous structure. Finally, the area was calculated using the "analyse particles" function of Fiji (settings: Size 50-30000 μ m², circularity 0-1).

After live imaging, cells and larvae were fixed in 4% PFA overnight at 4°C under agitation. Supernatants containing the larvae were collected and the larvae were pelleted using a bench centrifuge. Both cells and larvae were washed in PBS twice before being incubated in 250 μ L of PBS containing 1% donkey serum and 0.05% Triton X-100 for 24 h. The next day, cells and larvae were stained with primary antibodies for 1 h, washed then stained with secondary antibodies for 30 min. Following a final washing cells or larvae were placed in a 8 well μ -Slide (Ibidi®) and images were acquired and analyzed as described for the *ex vivo* skin samples.

NET Formation and Lifetime Assays

Neutrophils were isolated from human peripheral blood over Histopaque-/Percoll- gradient as described elsewhere (Aga et al., 2002). 2 \times 10⁵ neutrophils per well were plated in an 8 well μ -Slide (Ibidi®) in HBSS +Ca/Mg +10mM HEPES +3% plasma. Cells were stimulated with an MOI of 0.1 of *C. albicans* (SC5314 clinical isolate) pre-formed hyphae in the presence of 0.1 μ M SYTOX Green (Invitrogen, S7020) and in the absence or presence of 1, 10 or 100 μ g/mL of NES. Timelapse images were obtained every 10 min

for 14 h using a LEICA DMIRB microscope (20x objective) and analyzed using Fiji/ImageJ software. NET formation was counted dynamically over 14 h and NET lifetime was measured as the elapsed time until NET Sytox signal disappeared (events per 1500 cells per condition, 24 events per condition analyzed for NET lifetime).

To assess the potential of Nb-DNase II to degrade NETs, 28 000 neutrophils per well were plated in a 96 well plate in RPMI+10% serum in presence of 100 μ M PMA and 100 μ g of NES of DNase II for 3 h. Sytox Green was added at 1:1000 dilution prior to imaging by confocal imaging as described for the *ex vivo* skin samples.

NES Endonuclease Activity Assay

1 μ g of pMAL-c2X plasmid (size: 6700bp, Addgene, (Walker et al., 2010)) was incubated in the absence or presence of 1, 10 or 100 μ g/mL NES or 1 U/mL of DNase I (D5025, SIGMA) and in the absence or presence of 40 μ g/mL of G-actin (A2522, SIGMA) in HBSS +Ca/Mg +10 mM HEPES. After 15 or 45 min of incubation at 37°C, the samples were deactivated at 75°C for 5 min and 300 ng of DNA were analyzed via agarose electrophoresis.

Monocyte Viability Assay

Human peripheral blood monocytes were isolated over a Histopaque 1119 gradient (Sigma-Aldrich) and the CD14-positive monocytes isolated using MACS CD14 micro beads (Miltenyi Biotec) according to manufacturer's instructions. The CD14-positive monocytes were plated at 5×10^4 per well on an 8 well μ -Slide (Ibidi®) and neutrophils were plated at 2×10^5 per well on a 24 well plate in HBSS +Ca/Mg +10 mM HEPES +10% FCS. Neutrophils were then incubated in the absence or presence of NES (30 μ g/mL) and in the absence or presence of PMA (50 nM). After 5 h of incubation, the medium was transferred from the neutrophils onto the monocytes (after removal of the monocyte medium). Monocyte viability was quantitated 18 h later using 140–250 cells per condition with SYTOX green staining (0.1 μ M). Values were normalized against the viability of monocytes that had not received a medium change.

Protein Selection, RNA Extraction and cDNA Synthesis

For the screening of proteins secreted by *N. brasiliensis* L3 larvae (NbL3) with DNase activity, a Pfam analysis was performed on the NbL3 excretory/secretory products described previously (Sotillo et al., 2014) using HMMERv3.2 (Finn et al., 2011) to identify proteins containing a DNase domain.

Total RNA from *N. brasiliensis* was extracted using TRI reagent (Sigma-Aldrich, USA) as per manufacturer's instructions. Briefly, *N. brasiliensis* adult worms were homogenized in 500 μ L of TRI reagent for 2 min on ice using a pellet pestle followed by addition of 500 μ L of TRI reagent and incubated at RT for 5 min. Then, 0.2 mL of chloroform (Sigma-Aldrich, USA) was added, shaken vigorously for 15 s, incubated for 5 min at RT and pelleted at 12,000 *g* for 15 min at 4°C. The aqueous phase was transferred to a fresh clean tube and 0.5 mL of isopropyl alcohol (Sigma-Aldrich, USA) and 3 μ L of Glycoblue (Thermo Fisher Scientific, USA) was added. The mixture was mixed gently by inverting the sample 5 times, incubated for 10 min at RT and centrifuged at 12,000 *g* for 10 min at 4°C. The RNA pellet was washed with 1 mL of 75% ethanol in RNase-free water (Sigma-Aldrich, USA) and the pellet was air-dried. The RNA pellet was finally resuspended in 12 μ L of RNase-free water and kept at –80°C until use.

First strand cDNA was synthesized using reverse transcriptase as follows. One (1) μ L of oligo (dT) primers (500 μ g/mL) (Life Technologies, USA), 1 μ L dNTP mix (10 mM) (Bioline, UK) and 11 μ L of RNA were mixed and incubated at 65°C for 5 min in a 96-well thermal cycler (Applied Biosystems, USA) and on ice for 2 min. Then, 4 μ L (5x) of first strand buffer (Invitrogen, USA), 1 μ L 0.1 M dithiothreitol (Invitrogen, USA), 0.5 μ L RNaseOUT (40 units/ μ L) (Invitrogen, USA), 0.25 μ L (200 units) of SuperScript III reverse transcriptase (Invitrogen, USA) and 0.75 μ L water was added. Finally, the solution was incubated for 1 h at 55°C, then 15 min at 70°C in a thermal cycler and frozen at –20°C until use.

Gene Cloning

Cloning of *N. brasiliensis* cDNA Encoding for Nb-DNase II

The cDNA sequence encoding for the protein of interest (m.13872) was obtained from previous studies (Sotillo et al., 2014). The presence of a signal peptide was predicted using the online software SignalP v4.0 (<http://www.cbs.dtu.dk/services/SignalP/>, (Petersen et al., 2011)) and sequence without the signal peptide (amino acid residues 22–378) was amplified by PCR using the following oligonucleotide primers: Nb-m.13872F (5'-GCGCATATGGAATTCGGTCTGAGTTGCAAGAACATG-3') and Nb-m.13872R (5'-CGCCTCGAGGGCGGTTTTGTTTGTCTTCTT-3'); positions of start and stop codons are underlined.

The PCR reaction was performed as follows: 1 μ L (50 ng) adult worm cDNA, 3 μ L (10 μ M) each of forward primer and reverse primer, 10 μ L MyTaq red reaction buffer (Bioline, UK), 32.5 μ L water and 0.5 μ L MyTaq DNA polymerase (Bioline, UK). PCR conditions were 35 cycles of denaturation at 95°C for 15 sec, annealing at 50°C for 15 sec, extension at 72 °C for 45 sec, and final extension at 72 °C for 7 minutes. PCR products were subsequently digested with NdeI and XhoI (Biolabs, USA) to clone in frame into pET-41a (Novagen, USA). Recombinant plasmid was transformed into *E. coli* BL21 (DE3), plated onto Luria Bertani agar plates supplemented with 50 μ g/mL kanamycin (LBkan) and incubated overnight at 37°C. The recombinant clones were PCR amplified using T7 and reverse specific primers for confirmation of insertion of sequence.

Protein Expression

Expression of recombinant protein was induced by addition of isopropyl β -D-1-thiogalactopyranoside (IPTG) to 1 mM and cultured in LB supplemented with kanamycin for 24 h. The recombinant protein was located in inclusion bodies and purified as follows. Triton X-100 was added to a final concentration of 3% after sonication, the mixture incubated for 1 h at 4°C with gentle shaking and then

pelleted at 20,000 *g* for 20 min at 4°C. The supernatant was removed, the pellet washed twice with 30 mL of lysis buffer (with centrifugation at 20,000 *g* for 20 min at 4°C after each wash) and the final pellet resuspended in 20 mL of solubilization buffer (50 mM sodium phosphate, 40 mM imidazole, 300 mM NaCl and 8 M urea). The resuspension was incubated at 4°C overnight with gentle shaking, centrifuged at 20,000 *g* for 20 min at 4°C and the supernatant decanted and stored at –80°C.

Recombinant proteins were purified by immunoaffinity chromatography (IMAC) using 1 mL His-Trap Ni²⁺ columns using an AKTA Prime UPC FPLC system (GE Healthcare, USA) and eluted with an increasing linear gradient of imidazole (100–500 mM). Fractions containing purified recombinant proteins were combined and buffer exchanged into 1x PBS containing 300 mM NaCl and 8 M urea using a 3 kDa MWCO Amicon Ultra-15 centrifugal unit. The identity of expressed proteins was confirmed by SDS-PAGE and western blot using anti-His monoclonal antibodies.

Polyclonal Antibody Production

Male BALB/c mice were purchased from the Animal Resource Center, Perth, Australia and maintained at the AITHM animal facilities on the James Cook University, Cairns campus. Mice were kept in cages under controlled temperature and light with free access to pelleted food and water. All experimental procedures performed on animals in this study were approved by the James Cook University (JCU) animal ethics committee (A2433). All experiments were performed in accordance with the 2007 Australian Code of Practice for the Care and Use of Animals for Scientific Purposes and the 2001 Queensland Animal Care and Protection Act.

Three male BALB/c mice (6 weeks old) were immunized intraperitoneally with 50 µg of recombinant protein emulsified with 50 µl Alum adjuvant (Thermo Fisher Scientific, USA) and boosted twice at two weekly intervals using same amount of protein/adjuvant. Blood was collected at necropsy by cardiac puncture, allowed to clot and then serum was removed by centrifugation at 10,000 *g* for 10 min and kept at –20°C until use.

Homolog Identification and Phylogram Analysis

BlastP was used to identify protein sequences presenting high similarity to Nb-DNase II. Top-scoring hits with alignments covering at least 95% of the Nb proteins were considered for further analysis. A multiple sequence alignment was carried out using the alignment program MUSCLE using default parameters (Edgar, 2004). PhyML, a phylogeny software (Guindon et al., 2010), was used for a maximum-likelihood (ML) phylogenetic analyses of aminoacid sequences using approximate likelihood ratio test [aLRT] and Shimodaira–Hasegawa [SH]-aLRT for a fast-approximate likelihood-based measure of branch support and Nearest-neighbor interchanges (NNI) for tree improvement. The tree was finally visualized with The Interactive Tree of Life (iTOL) online phylogeny tool (<https://itol.embl.de/>, (Letunic and Bork, 2019)). For identification of putative Nb-DNase II homolog in Na, all sequences annotated in the genome (Tang et al., 2014) with a DNase motif were aligned to Nb-DNase II with Clustal Omega. The Multiple sequence alignments were visualized using the JalView 2 Desktop application (<http://bioinformatics.oxfordjournals.org/content/25/9/1189>). Finally, sequence features of interest were manually highlighted in the alignments.

QUANTIFICATION AND STATISTICAL ANALYSIS

The choice of statistical tests was based on sample size and on Bartlett's test when normal distributions of the errors were expected. Data from separate experiments were pooled when possible. Statistical parameters including the exact value of *n*, the definition of center, dispersion and precision measures (mean ± SEM) and statistical significance are reported in the Figures and Figure Legends.

Representation and data analysis were performed GraphPad Prism 8. Statistically significant values are indicated as follows: NS, *p* > 0.05; *, *p* < 0.05; **, *p* < 0.01; ***, *p* < 0.001. Spearman's rank correlation statistical analysis was performed using Minitab 17 Statistical Software (2010). Of note, when multiple comparisons were performed in post hoc test, the comparisons reported on the figure are the only one that had been tested.

DATA AND CODE AVAILABILITY

The protein sequence of the DNase II from *Nippostrongylus brasiliensis* identified in this work is available in [Data S1](#) and has been deposited in GenBank, accession code MN938457.

The macro designed to quantify the distance of neutrophils and monocytes to the larvae is detailed in concept in [Figure S2](#) and has been available through Zenodo, <https://doi.org/10.5281/zenodo.3596520>.

All other original/source data for this paper are available from the corresponding author on request.